AMERICAN UNIVERSITY OF BEIRUT

EFFECT OF SOIL DAMPING IN SOIL-STRUCTURE INTERACTION ON THE SEISMIC DESIGN OF REINFORCED CONCRETE BUILDINGS

by
TAMARA CHAWKI WEHBE

A thesis
submitted in partial fulfillment of the requirements
for the degree of Master of Engineering
to the Department of Civil and Environmental Engineering
of the Maroun Semaan Faculty of Engineering and Architecture
at the American University of Beirut

Beirut, Lebanon
April, 2022

AMERICAN UNIVERSITY OF BEIRUT

EFFECT OF SOIL DAMPING IN SOIL-STRUCTURE INTERACTION ON THE SEISMIC DESIGN OF REINFORCEDCONCRETE BUILDINGS

by

TAMARA CHAWKI WEHBE

Approved by:

George A. Saad

Dr. George Saad, Associate Professor

AdvisorCivil and Environmental Engineering

Dr. Shadi Najjar, Associate Professor Co-Advisor
Civil and Environmental Engineering

Dr. Salah Sadek, Professor Member of
CommitteeCivil and Environmental Engineering

Date of thesis defense: April, 2022

AMERICAN UNIVERSITY OF BEIRUT

THESIS RELEASE FORM

Student Name: ____Wehbe_____Tamara_____Chawki_____
Last First Middle

I authorize the American University of Beirut, to: (a) reproduce hard or electronic copies of my thesis; (b) include such copies in the archives and digital repositories of the University; and (c) make freely available such copies to third parties for research or educational purposes:

☒ As of the date of submission

☐ One year from the date of submission of my thesis.

☐ Two years from the date of submission of my thesis.

☐ Three years from the date of submission of my thesis.

_____4/4/2022_____

Signature Date

ACKNOWLEDGEMENTS

Throughout the process of preparing this dissertation I have received tons of support, assistance, and guidance. Therefore, I would like to take this chance to express my deepest gratitude to those who left their valuable fingerprints on myself hence my work.

Firstly, my supervisors, Dr. George Saad, and Dr. Shadi Najjar, whose insightful feedbacks pushed me to sharpen my thinking and whose expertise bought my work to a higher level. I would also like to acknowledge Dr. Salah Sadek from the thesis committee for his valuable input.

To my friends: Mona, Fatima and Shahin; your constant support kept me going. Thank you for always being there.

Most importantly, I want to dedicate this to the two behind it all: Mom and Dad, all that I have achieved and will achieve is because of you and for you. And finally, my deepest gratitude is to my brother Ahmad who have always been the virtual shoulder I lean at.

ABSTRACT

OF THE THESIS OF

Tamara Chawki Wehbe for Master of Engineering
Major: Civil Engineering

Title: Effect of Soil Damping in Soil-Structure Interaction on the Seismic Design of Reinforced Concrete Buildings

The main objective of this research is to contribute to a quantification of the effect of soil damping within the soil-structure interaction framework on the seismic design of reinforced concrete structures. For this purpose, a model that compiles all factors to be considered in a soil–structure interaction problem was developed. The physical model of the structure is based on a slender reinforced concrete building with underground stories, lying on dense sand in a case and on loose sand in another. This model is subjected to earthquake input signal and modelled using Plaxis finite element analysis software. The HS-Small constitutive soil model in Plaxis was adopted to represent the soil's hardening behavior when subjected to earthquakes. Hysteretic, Rayleigh, radiation and numerical damping were introduced into the numerical model and their influence was analyzed. The seismic load was incorporated by the ground acceleration record of Loma Prieta earthquake and simulated in Plaxis in terms of horizontal prescribed displacements. The results obtained lead to a direct assessment of the importance of including damping and how it alters the seismic design of reinforced concrete buildings. These results can be illustrated in terms of the effect damping has on the lateral displacements and design base shear of the superstructures and the lateral earth pressure on the retaining walls as well as the horizontal pressures of the soil elements. In addition, this research item provides the calculation method required to accurately incorporate damping coefficients in numerical modelling.

Keywords: Soil-structure interaction, damping, hardening soil behavior, HS-small constitutive model, finite element analysis

TABLE OF CONTENTS

ILLUSTRATIONS

Figure

TABLES

Tables

CHAPTER 1
INTRODUCTION

1.1. Background

In daily life, engineers usually overlook the effect of soil-structure interaction (SSI) by cropping the building at ground level and assuming a fixed base. According to research, the fixed base assumption turned out to be inappropriate specifically for structural systems with stiff vertical elements used for lateral systems like shear walls. This is unsuitable as these structures are sensitive to small rotational and translational movements that are ignored by assuming a fixed base model (Ahmadi, Khoshnoudian, & Hosseini, 2015). While considering soil structure interaction, the increase of the overall damping taking place caused by dynamic soil-structure interaction is always beneficial, while the increase of the overall flexibility (due to the compliance of the foundation) may be either positive or negative depending on the relationship between the characteristics of the structure, the soil layer(s) and the seismic excitation(s) (Tsompanakis, Psarropoulos, & Katsirakis, 2021). However, by including the underground stories, the effect of soil-structure interaction is simulated which consequently influences structural responses in two different mechanisms. The first mechanism, Kinematic SSI, which is due to the presence of stiff elements in the foundation soil, causes the input motion to completely deviate from the free-field motion which, as a result, filters the ground motion experienced by the structure (FEMA, 2005). This is done via the foundation's flexibility and soil damping. An abundant amount of research was conducted to illustrate the importance of incorporating soil-structure interaction (Dutta & Roy, A critical review on idealization and modeling for interaction among soil–foundation–structure system, 2002) (Dutta, Bhattacharya, & Roy,2004) (Rayhani & El Naggar, 2008) (El Ganainy & El

Naggar, 2009) (Mekki, Elachachi, Breysse, Nedjar, & Zoutat, 2014) (Tabatabaiefar, Fatahi, Ghabraie, & Zou, 2015) (Saad, Najjar, & Seddik, 2016) (Cruz & Miranda, 2017) (Jaber L. , Temsah, El-Mossallamy, & Hajj Chehade, 2019) for example, but few discussed the vital method of introducing soil damping into their numerical models (Ambrosini, 2006) (Boaga, Renzi, Deiana, & Cassiani, 2015) (Jaber L. , Temsah, El-Mossallamy, & Hajj Chehade, 2018) (Rayhani & El Naggar, 2008) for example. It is crucial for the literature to extensively describe such methods revolving around the introduction and inclusion of soil damping as these practices can have a significant effect on capturing the soil-structure interaction accurately. Hysteretic and Rayleigh damping respectively account for the energy dissipation due to friction between soil elements and soil flexibility (Mylonakis & Gazetas, 2000), which affects the structural response of any structure under analysis. As such, the purpose of my research is to studying soil's damping influence on soil structure interaction under earthquakes using Plaxis2D and how it affects the seismic design of reinforced concrete elements. To effectively achieve this purpose, a methodology was developed to calculate soil damping coefficients using Plaxis 2D dynamic features.

1.2. Statement of the problem

The effect of soil-structure interaction on the seismic response of structures has been widely addressed in the literature. Studies tried to gather the possible effects of modelling structures with underground stories rather than cropping structures at their base (considering a fixed base). Emphasis has been given on the physical modeling of soil media, since it appeared that the modeling of the building is rather straightforward. Different approaches were used to model the soil-media, such as impedance functions

(Mekki, Elachachi, Breysse, Nedjar, & Zoutat, 2014), simulating soil as springs (Saad, Najjar, & Seddik, 2016) or dashpots (Cruz & Miranda, 2017), constant damping percentage (Dutta, Bhattacharya, & Roy, 2004), nonlinear hysteretic damping model by Wolf 1994 (Jaber L. , Temsah, El-Mossallamy, & Hajj Chehade, 2019) and reduction curves (El Ganainy & El Naggar, 2009). However, these techniques don't take into consideration all soil properties therefore don't grasp the accurate soil behavior, especially under small strains, earthquakes for example.

Starting from the available models in the literature, this study aims at providing a framework for the analysis of reinforced concrete buildings with underground stories during earthquakes. For this purpose, a numerical model was built the compiles the three aspects of the problem: structural, geotechnical and earthquake features. The presented approach relies on the hardening soil model available in Plaxis 2D for capturing the nonlinear behavior of soil elements under earthquakes and Seismosignal software tool for the demonstration of the Earthquake characteristics. Moreover, different published research items were used to calculate soil mechanical and damping properties.

Consequently, this approach provides a closer look on how soil damping affects the seismic design of buildings and an alternative accurate mean of inputting soil damping characteristic into numerical models.

1.3. Project motivation

The aim of this research is to develop a framework for the input of different damping coefficients in numerical models that incorporate soil-structure interaction. However, no attempts have been made in the literature to demonstrate the influence of damping on the seismic design of reinforced concrete buildings using numerical modeling

approaches. Therefore, this study will be devoted to assessing the effect of the inclusion of different sources of damping on the seismic response of reinforced concrete buildings. This objective will be achieved by modelling a reinforced concrete building with basement walls placed over a 150m-by-30m sand medium and subjected to an earthquake using Plaxis 2D FEA software. HS-Small constitutive soil model will be used to capture the granular soil's non-linear behavior decomposition. And Loma Prieta Earthquake input signal will be implemented using an acceleration-time history simulated as prescribed displacements which will then be increased to three times the originally induced earthquake motion. Finally, results will be used to assess the structural base shear, moment demand and deflections associated with the building. In addition to the structural response, results will also discuss the lateral earth pressures. Moreover, results will also assess the role of each type of damping has in soil-structure interaction in terms of significance.

This would enable engineers to determine the effect of damping on the seismic base shear, lateral displacements, and effective stresses which in most cases, is a favorable effect as it leads to more economical structural designs. Moreover, it provides engineers or future researchers with a clear demonstration of the input required to accurately include all required parameters for a numerical model that encompasses a soil-structure interaction problem. This will hence, illustrate the importance of including soil damping in the analysis and how disregarding it affects both geotechnical and structural aspects of the analysis.

1.4. Thesis structure

The structure of this thesis is broken down to five chapters: the introduction which includes the literature review, the statement of the problem and the motivation behind this research, this presents a general overview of the problem. The second chapter provides different approaches used to address the problem. The third chapter discusses the methodology used to achieve this thesis's goals: a numerical model where the modelling steps will be explained in detail. The fourth chapter which presents the outcome of this research item. The fifth and last chapter discusses the results provided and states the conclusion alongside recommended future work.

CHAPTER 2

LITERATURE REVIEW

2.1 Introduction

A significant amount of research items has focused on the importance of the inclusion of soil-structure interaction effects within the structural and geotechnical engineering analysis and design framework. For this purpose, these research attempts provided a variety of techniques, mathematical models, and modelling approaches to demonstrate all variables to be consider in the analysis. However, only few addressed the effect of damping coefficients in the context of a damping constant percentage, mathematical functions, or a damping ratio etc. To better illustrate this, the following mentioned research items will provide better explanation of the approaches used previously that made up the foundation of this current research item.

2.2 Background

(Dutta, Bhattacharya, & Roy, 2004) aimed at identifying the influential parameters which can regulate the effect of soil-structure interaction on the change of base shear of low-rise building frames in both the elastic and inelastic range responses of buildings. The three-dimensional space frames were modelled using two nodded frame elements along with four nodded plate elements, with brick in-fill, that aims at resisting lateral forces due to ground excitation (Figure 1). All these buildings were modelled with and without tie-beams, to consider the effect of including them.

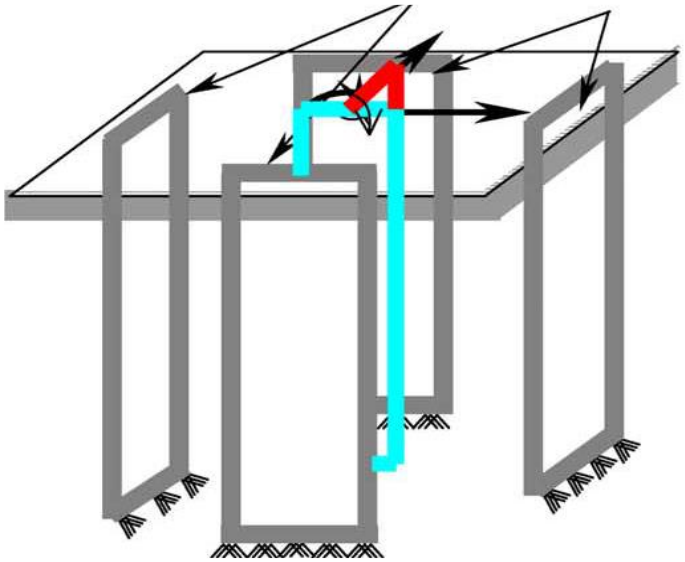

Figure 1 Idealized representation of low-rise building used to analyze inelastic range behavior

Within these researchers' method, the Finite element method was adopted to formulate the mass and stiffness matrices for the building frames. Soil media was simulated by the use of springs that resembled clay soil. However, soil Rayleigh and hysteretic damping was incorporated by considering 5% of critical damping in each mode of vibration. Moreover, the structural response under ground excitation was obtained from step-by-step integration while elastic range behavior was analyzed using the nonlinear equations of motion for the structures by Newmark's b-g method with modified Newton–Raphson technique. The variables considered within this research study were types of clay, number of stories, and number of bays. The results encompassed the effects of these variables on the ratio of column to beam stiffness, frequency on soil-flexibility, ductility demand and hysteretic energy demand. Results showed that the effect of soil-structure interaction plays a significant role in increasing the seismic base shear of dwarf structures. However, it may also decrease the seismic response of slender structures which is illustrated in Figure 2.

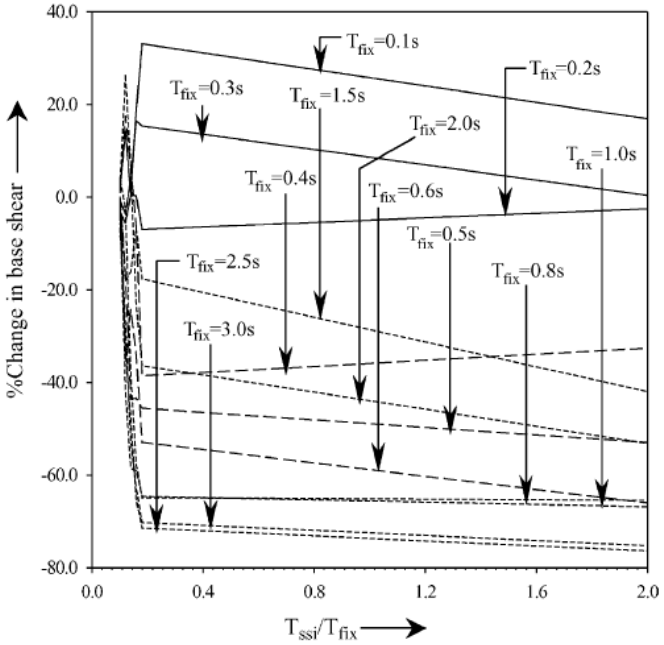

Figure 2 Variation in base shear for single storey plane frame with various lateral natural periods due to El-Centro Earthquake

In which, (Tfix) is the lateral natural periods of the systems at fixed base condition and (Tssi) is the natural period at flexible base condition.

Another study by (El Ganainy & El Naggar, 2009) investigated the seismic performance of moment-resisting steel buildings with underground stories. Soil parameters corresponding to soil type C (firm soil) and soil type E (soft soil) were used in the analysis. The nonlinear structural analysis program Perform 3D was used to conduct the performance assessment of five, ten and fifteen storey buildings, with underground stories (ranging from zero to five) in the context of performance-based design. The building structures were numerically modelled using Etabs. Rayleigh damping through the foundation was neglected while the hysteretic damping was included via backbone curves that build on the lateral pressure-lateral deflection relationship. Moreover, soil damping was calculated using DEEPSOIL by applying the

G/Gmax modulus reduction curve and the equivalent damping ratio versus shear strain relationship. Results were expressed by the envelope of the storey shear and that of moment demand on the buildings throughout the earthquake events and by the maximum usage ratio of the limit states defining the performance level of the structural components of the building. It was seen that SSI decreased the base shear and moment demands on buildings founded on stiff soil but increased these parameters on buildings founded on soft soil as can be seen in Figures 3 and 4. Contrary to common belief, this increase in base shear and moment demands on structures built on soft soil shows us that SSI effects are not favorable in every case. As such, these results have re-iterated the significance of incorporating SSI. However, they have also shown us the vitality of further investigating the effects of SSI before implementing it.

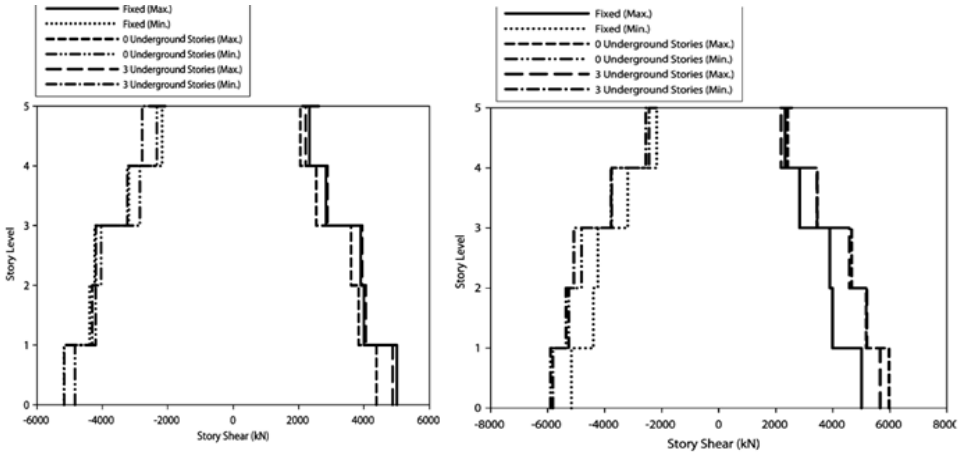

Figure 3 Storey shear demand on five storey buildings Left-Soil C, Right-Soil E)

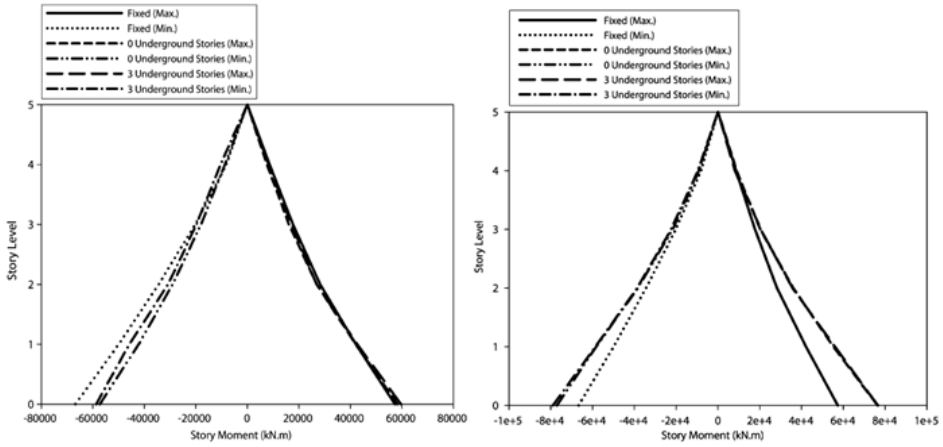

Figure 4 Storey moment demand on five storey buildings (Left-Soil C, Right-Soil E)

Similar to the abovementioned studies, (Mekki, Elachachi, Breysse, Nedjar, & Zoutat, 2014) investigated the seismic performance of reinforced concrete structures while considering the soil-structure interaction. To meet this objective, the N2 approach was used. This approach relies on two critical assumptions that consequently limit its uses. The first assumption is that the displacement shape is constant, which means that it does not change during the structural response to ground motion. Secondly, the first mode is predominant. The N2 approach concept is based on determining the capacity curve of a fixed base system oscillating predominantly in the first mode, which is then modified to obtain the capacity curve of a flexible base system by using the nonlinear replacement oscillator concept. Moreover, the soil-structure interaction is introduced through impedance functions. These functions describe the stiffness and damping characteristics of the foundation-soil system. The impedance functions are represented by their corresponding lateral and rotational springs or dashpots that are represented by stiffness and damping properties. Therefore, soil-structure interaction was simulated by the use of springs and damping was introduced by an effective damping percentage that accounts for both soil material and radiation damping. This study confirmed that an increase in damping occurs when the effect of the SSI is taken into account, which will result in a

reduction in seismic demand due to the dissipation of energy through soil radiation and internal damping. This is demonstrated in Figures 6 and 7. These two effects occur simultaneously during the seismic movement. It is thus very difficult to ignore the influence of these two phenomena.

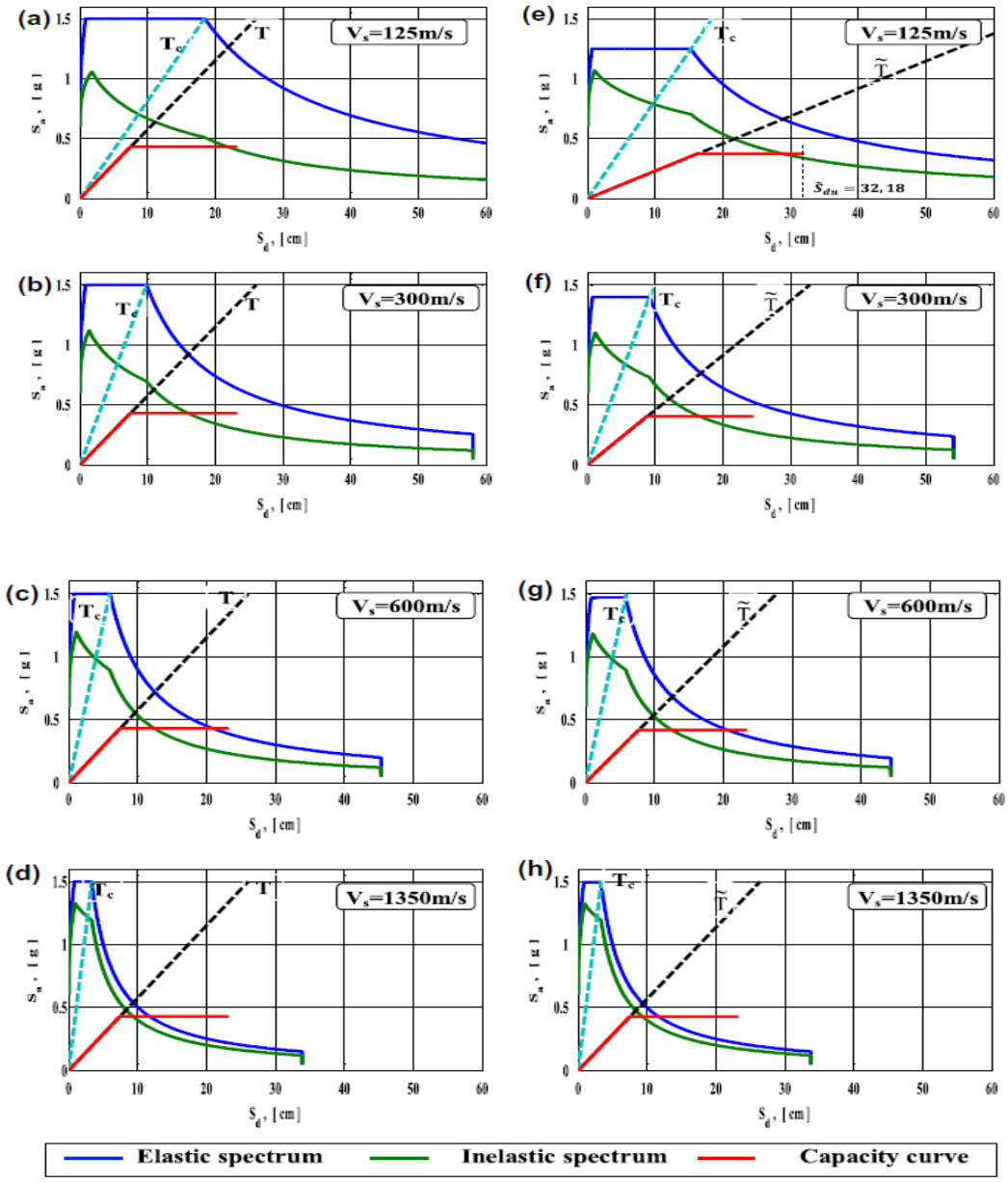

Figure 5 Capacity and demand spectra for different values of soil shear wave velocities: without SSI (left) and with SSI (right) (PGA = .6 g).

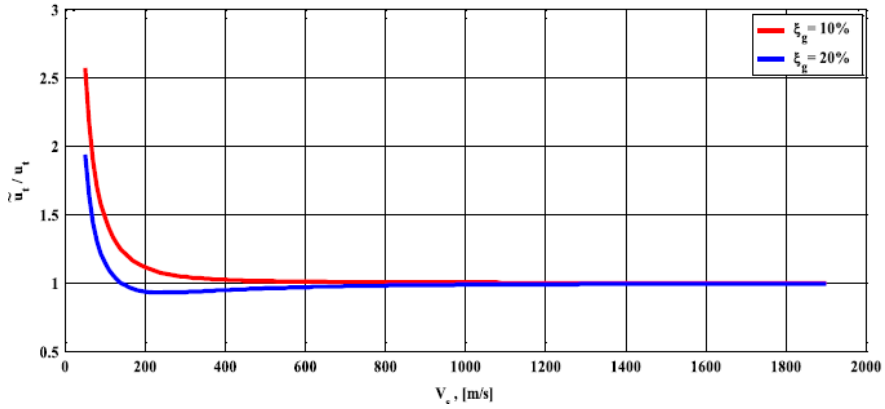

Figure 6 Variation of ~ut=ut with Vs for different soil damping Eg (case study).

In addition to studying the effect of underground stories, (Ahmadi, Khoshnoudian, & Hosseini, 2015) also focused on studying the role of soil material damping within engineering demand parameters. This objective was accomplished by modelling a superstructure as a two-dimensional nonlinear multi storey building. The superstructure model is based on the structural modeling approach suggested by FEMA 440, 2005. This code of practice allows engineers to simulate complex structures by equivalent MDOF models which are termed stick models. These can be seen in Figure 7 which shows the soil-structure model. Further, the soil beneath was replicated according to the cone model. This cone concept represents the soil underlying the foundation by a homogenous half-space medium, thus simplifying this system by a 3-DOF one. Moreover, the soil's complex behavior was made simpler by simulating it using dashpots and springs constants.

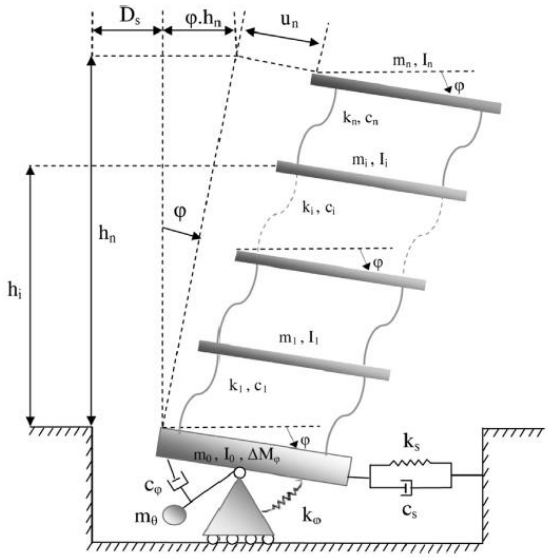

Figure 7 Soil-Structure Simulation Model

In figure 7, mi and Ii stand for the mass and the mass moment of inertia around the geometric center of the ith storey.

However, the flexibility of the foundation was not taken into consideration and the inertial part of the soil-structure interaction was only considered. The effects of various parameters were evaluated using the relative reduction ratios between demands in the presence of soil material damping and, in its absence, –thus including radiation damping only. Soil material damping was incorporated using the nonlinear hysteretic damping model by Wolf in 1994. This material damping type is employed in the paper by reducing the spring and dashpot forces using the following equations:

$$P_k = k_{s,\varphi}|u_0 - u_1| \ \tan\ \delta \mathrm{sgn}(\dot{u}_0 - \dot{u}_1)$$

$$P_C = C_{s,\varphi}\overline{\left|\dot{u}_0 - \dot{u}_1\right|}\,0.5\ \tan\ \delta \mathrm{sgn}(\ddot{u}_0 - \ddot{u}_1)$$

In these formulas, tan δ=2μs where δ=friction angle and μs is the material damping of the soil. In addition, μ0 and μ1 and their derivatives are the difference in the displacements and velocities produced in the spring and dashpot in a specific time

interval. Finally, Pk and PC are transverse forces corresponding to the spring and dashpots, respectively.

Given the above, results demonstrated that as the number of stories increases, the effects of soil material damping on the responses become more pronounced. Moreover, in the case of slender structures and higher structural ductility, the effects of soil material damping are influential in comparison to those of radiation damping. Generally, the consequences of soil material damping on the displacement demands are greater than those on the force demands. Furthermore, the roof displacement demands of the superstructure are more affected than the maximum storey drift angle response by soil material damping.

Also, (Saad, Najjar, & Seddik, 2016) investigated the behavior of reinforced concrete shear wall buildings with underground stories under seismic loadings. The buildings were numerically modeled with a fixed-base, flexible base and with an incrementally increasing number of underground stories as observed in figure 8. The models were analyzed under two subsurface conditions- very dense sand and moderate dense sand- and three earthquake input motions.

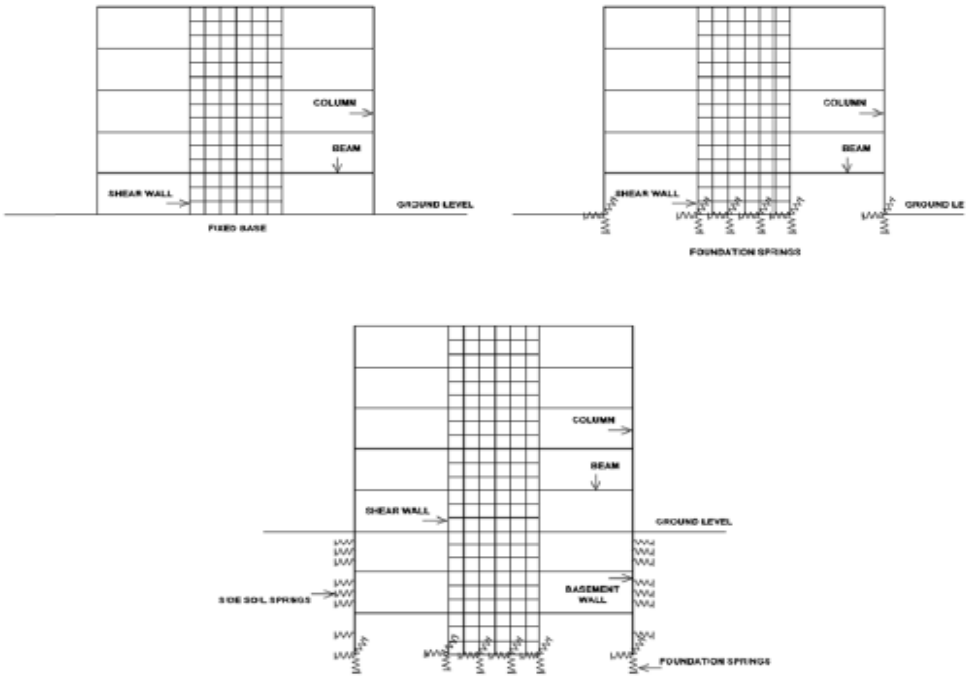

Figure 8 The mathematical models used for the analyses of the different building models; fixed base case (upper left), flexible base (upper right) and three basements (lower middle)

The multi-linear kinematic plastic link theory of SAP2000 was used to simulate the soil structure interaction effects, considering the non-linear approach. As a result, side soil was modelled as non-linear springs described by a hysteretic lateral pressure versus lateral displacement relationship that is consistent with the commonly used P-Y method. Moreover, to account for the degradation of stiffness in the spring's unloading-reloading cycles, reduced equivalent nonlinear stiffnesses for the springs were used. Soil-structure interaction at the foundation was simulated by equivalent linear springs that represented the associated foundation stiffnesses at different degrees of freedom. These springs accounted for energy dissipation during soil-structure interaction. The study discussed the effect of altering several variables: the inclusion of soil-structure interaction, distinct soil types, different earthquake characteristics on the seismic response of 5-storey buildings, and the number of above ground stories on the seismic

response of the structures. Results had shown that the effect of soil-structure interaction is not only significant but leads to governing storey shear demands in low-rise structures. However, it also concluded that storey shear demands decrease by incorporating soil-structure interaction in high-rise structures.

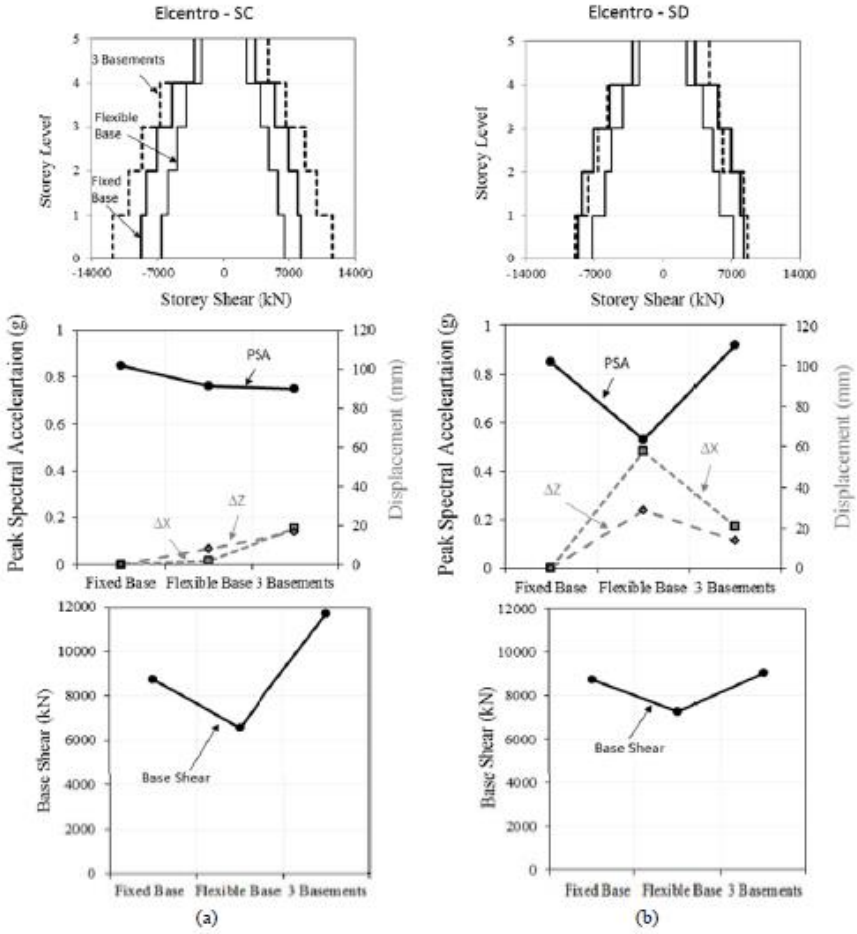

Figure 9 Variation of storey shear demands, attracted spectral acceleration, structure's vertical and horizontal displacements at ground level, and base shear at instant of peak load demand of 5 story buildings subjected to El-Centro earthquake for a) soil class C and b) soil class D

In a similar manner to (Saad, Najjar, & Seddik, 2016), (Cruz & Miranda, 2017) modelled soil-structure interaction in buildings but focused on its effect on damping ratios. The numerical model encompassed buildings with circular rigid foundations sitting on elastic half-space. To investigate this, transfer functions of the horizontal absolute

accelerations were developed in the frequency domain. An optimization procedure for finding the effective modal periods, damping ratios, and mode shapes that minimize the ordinates of the transfer functions was used. These transfer functions, which were derived based on the dynamic response of a fixed-base structure, were used to obtain an equivalent estimate of the dynamic response of a building with a flexible base. Similar to previous research soil-structure interaction was simulated by dashpots. Moreover, soil damping was interpreted in the form of damping modal ratios where hysteretic damping was not considered. This research leads to several conclusions. Firstly, as the wave parameter decreases, the effects of soil structure interaction become more significant. In addition, the effective damping ratio of the fundamental period of vibration increases as its corresponding height and aspect ratio decreases, because of soil-structure interaction. However, soil-structure interaction effects tend to reduce the effective damping ratio of the fundamental period of vibration in slender structures leading to a fixed base realization as noticed in figure 10. Moreover, damping ratios increase with the decrease of wave numbers. A significant finding is that the effective modal damping ratios of modes that have significant contributions to the seismic response of buildings show an approximate linear increase with the increase in frequency as seen in figure 11. The conclusions were of high importance as they state that stiffness proportional damping models are more appropriate to capture radiation damping in buildings.

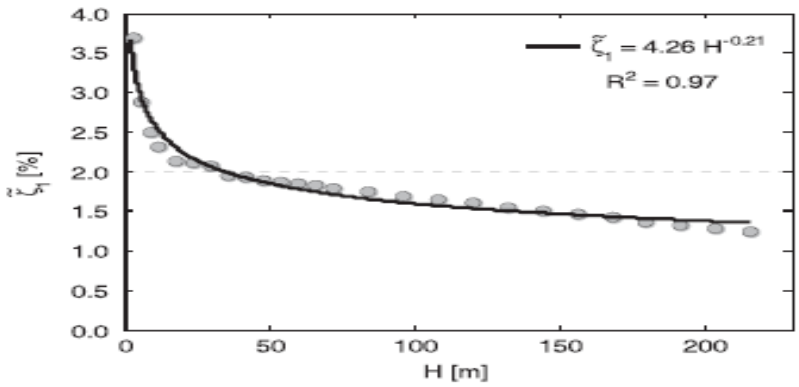

Figure 10 Variation of the effective damping ratio of the fundamental mode with building

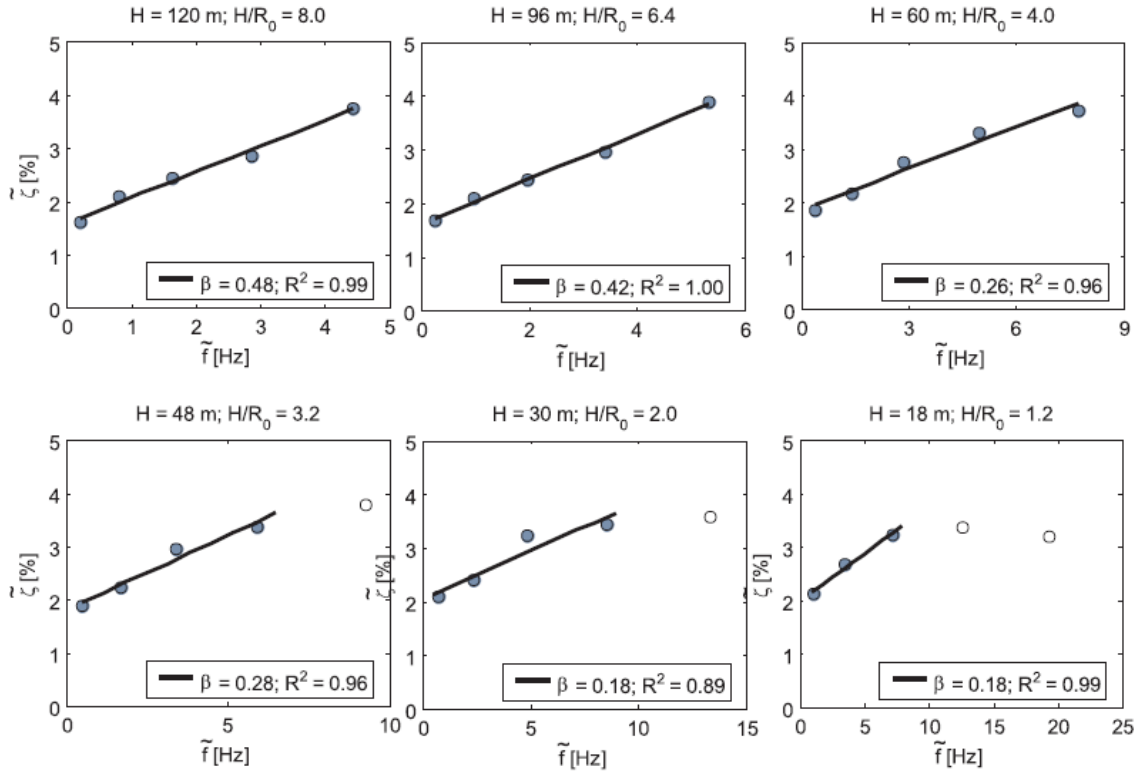

Figure 11 Variation of the effective damping ratio for increasing effective modal frequency

Not only the previous researchers but also (Khosravikia, Mahsuli, & Ghannad, 2018) evaluated the effect of soil-structure interaction (SSI) on the seismic risk of building structures but used an alternative approach. The researchers approached their study from a probabilistic perspective by using Montecarlo simulations where they computed the probability distribution of the seismic loss for fixed-base and flexible-base structures or stiff and soft structures. To compute this probability distribution; the soil-foundation substructure was simulated using a discrete model which is illustrated in figure 12. The variables involved in building this model are the frequency dependent sway (u), rock stiffness (k) and the sum of both material and radiation damping. The

conclusion of the analysis was various probability ranges that categorized SSI effect as beneficial, unimportant, or detrimental to various structures, represented by $P(l_{flex} \leq 0.9l_{fix})$, $P(l_{flex} \leq l_{fix})$ and $P(l_{flex} \leq 1.1l_{fix})$. In addition, this research concluded that SSI is likely to reduce both drift and acceleration responses as the number of stories increases, which means that taller buildings benefit more from the reduction of responses due to SSI. Moreover, the results for buildings on very soft soil were in line with the common belief that SSI has a favorable effect. However, the results for buildings on moderately soft soil reveal a considerable probability, up to 0.4, that SSI has an adverse effect on the structure and increases the seismic losses.

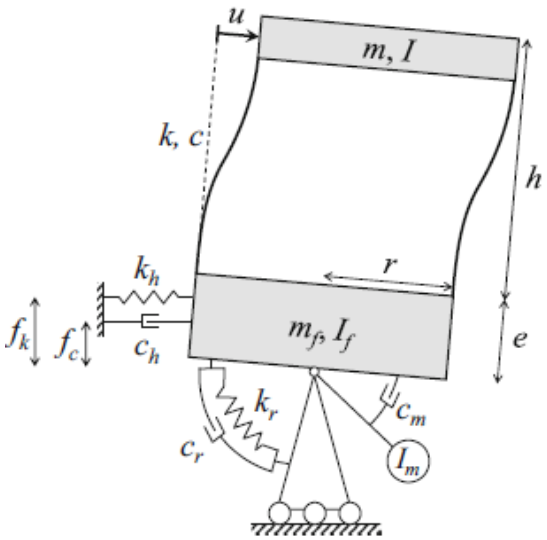

Figure 12 Discrete model used in the analysis

Within the same framework, a recent study by (Jaber L. , Temsah, El-Mossallamy, & Hajj Chehade, 2019) investigated the effect of underground stories on the dynamic response of buildings, particularly high-rise structures. For their purpose, the researchers used Plaxis 2D as a tool to model these buildings. The general numerical model was a replica of a reinforced concrete slender building overlying loose soil which was subjected

to an earthquake as observed in Figure 11. Most importantly, soil damping was simulated by considering both Rayleigh and hysteretic damping. Rayleigh damping was introduced by calculating the damping coefficients α and β whereas hysteretic damping was accounted for by the parameters Go and $\gamma_{0.7}$. The small strain hardening constitutive model was used to simulate soil's behavior when subjected to earthquakes. The numerical models used were three slender buildings (symbolized as S3, S4, and S6) with twelve, sixteen and twenty-four stories (H=36, 48 and 72m), each holding a height to base width ratio of 3, 4 and 6 respectively. Each building was analyzed with zero, one, three and five underground stories (symbolized as B0, B1, B3 and B5). An earthquake input motion was imposed on the buildings individually and the analysis in the time domain was based on Newmark 1959, which is Newmark's implicit time integration equations that are embedded in Plaxis. Results discussed the effect of underground stories on soil horizontal displacements at different depths, roof's lateral displacements, base shear forces and the maximum moments. The study concluded that as the number of underground stories increases, the displacements at the building base, the base shear forces and maximum moments decreased simultaneously which consequently improved the building's stability. This conclusion is displayed in Table 1 which shows the reduction in base shear and moment demands obtained for the different buildings S3, S4 and S6 with varying underground stories B0, B1, B3 and B5. Moreover, it also proved that it is crucial to incorporate soil-structure interaction when analyzing structures founded on loose soils.

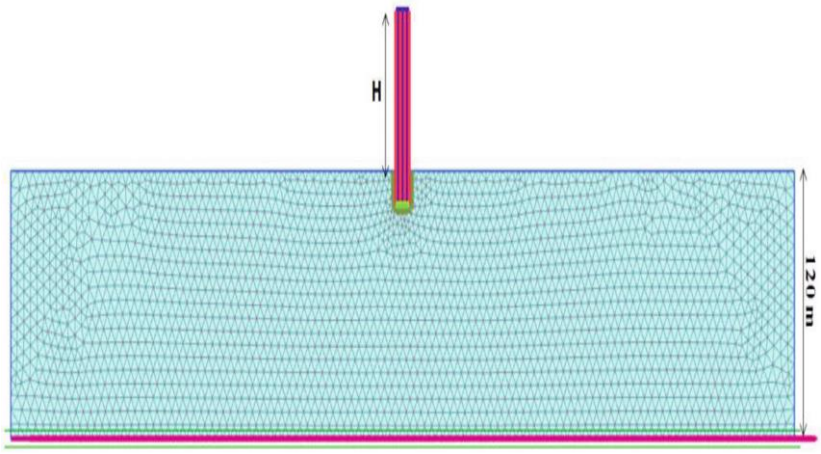

Figure 13 Two-dimensional finite element soil-structure interaction model

Table 1 *Base shear forces and moments and their rate of reduction function of the number of stories*

	Base shear (KN)	Reduction%	Moment (KN.m)	Reduction%
S3B0	76.98	-	186	-
S3B1	28	63.63	24.1	87.04
S3B3	5.66	92.65	13	93.01
S3B5	3.33	95.68	12.5	93.28
S4B0	153.6	-	405.5	-
S4B1	73.3	52.28	33	91.86
S4B3	8.07	94.75	21.26	94.76
S4B5	5.77	96.25	16.61	95.9
S6B0	-	-	-	-
S6B1	201.29	-	37.2	-
S6B3	11.81	-	44.95	-
S6B5	13.27	-	60.82	-

2.3 Conclusion

The provided research demonstrated several methods directed towards one conclusion, the importance of including soil-structure interaction in the seismic analysis of buildings. Several approaches were used to reach this outcome by simulating different soil-structure interaction models both experimentally and numerically. Moreover, different attempts were made on a suitable yet realistic approach to include soil damping as results proved the effect dissipation of energy has on the seismic response of structures.

Furthermore, these research items shared some common findings discussed below:

1- Several methods can be used to incorporate soil-structure interaction whereas only few can accurately include all variables that must be considered in an analysis.
2- The effects of soil-structure interaction are crucial in buildings founded on loose soils whereas are less important when considering structures on dense soils.
3- Soil-structure interaction effects doesn’t only affect displacements but also plays a significant role in altering shear and moment demands of the structural systems
4- There are several means to incorporate damping in soil-structure interaction, but a way to incorporate all forms of damping is yet to be researched about.

CHAPTER 3

NUMERICAL MODEL

3.1 Introduction

This chapter provides a brief explanation of the modelling techniques and steps used to build up the numerical model. This numerical model is made up of a fifteen-story building with three underground stories, subjected to an earthquake loading applied on the bed rock as shown in Figure 14. The Hardening Soil-Small Strain model implemented in Plaxis is used to accurately simulate soil's behavior under unloading-reloading cycles. Four types of damping have been addressed and imposed within the numerical model. Seismosignal is used to simulate the imposed earthquake properties and present as an outcome the acceleration-time history which is inputted into Plaxis. The Earthquake motion is resembled as prescribed displacement in Plaxis. Plate and node-to-node elements are used to model the walls/slabs and columns, respectively. The analysis has been conducted under different phases of construction. Time steps and sub steps are taken into consideration and their mean of calculation is discussed within this chapter.

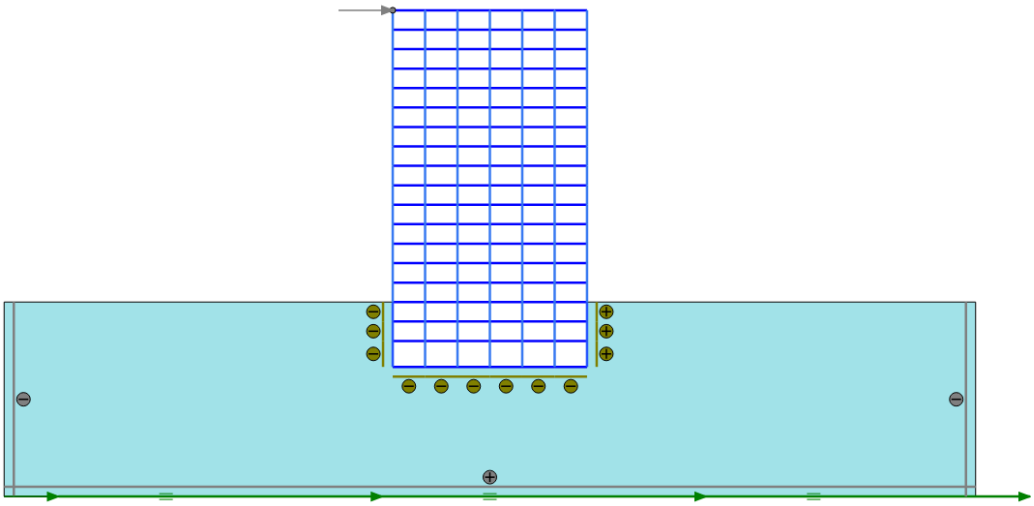

Figure 14 Numerical Model

3.2 Model Type and Soil Element Type

In Plaxis 2D, the numerical elements may be modelled either by a plane strain or an axisymmetric model. A building subjected to an earthquake is best modelled by a plane-strain which allows for the use of free-field boundary conditions that will be explained later in this item. However, the plane strain model is generally used in case of structures where one of the dimensions is very large as compared to the others. Figure 15 provides a clear understanding of the two model types.

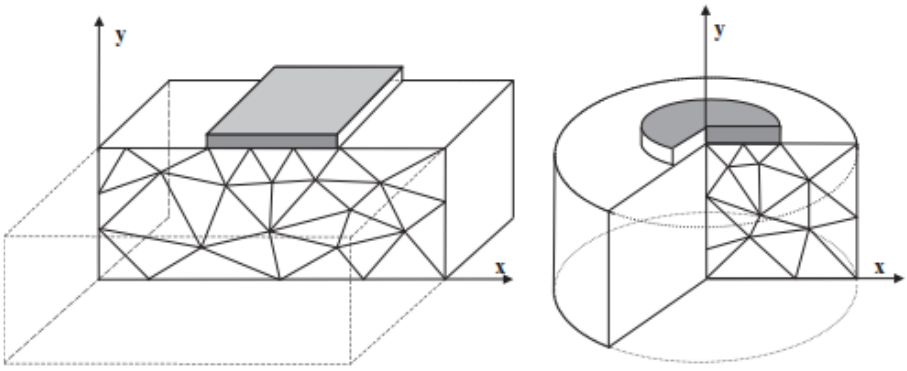

Figure 15 Difference between a plane strain (left) and axisymmetric problem (right)

In Plaxis 2D, a choice of either a 15-node triangular element or a 6-node triangular element is available. The 15-node element provides a fourth order interpolation for displacements and the numerical integration involves 12 Gaussian points (stress points) while the 6-node element provides a second order interpolation for displacements and the numerical integration involves 3 Gaussian points. It is important to note that failure loads or safety factors are generally over predicted using the 6-noded elements. Furthermore, the 15-node element is particularly recommended for axisymmetric analysis even though it consumes more memory and exhibits slower calculation and operation performance.

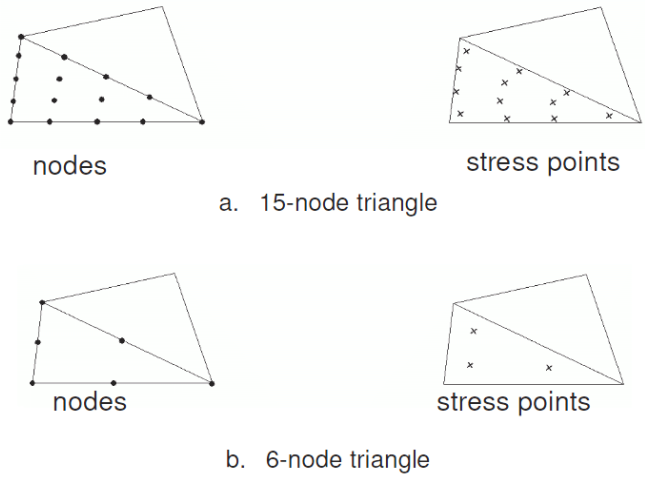

Figure 16 Difference between 15-noded elements and 6-noded elements

3.3 Model Boundaries

Within the literature, researchers do not normally justify why they opted for their choice of the horizontal and vertical boundary limits which they used in their numerical models. However, it's crucial for this research to justify the choice of the boundary limits to further explain how an alteration in the boundary limits affects the numerical model. As such, a sensitivity analysis was conducted to understand how results are changed with the change of both the model width and depth. For the model depth, the numerical model was at first built using a model which is 100m deep which then was modified to 150m and 50m respectively. Knowing that Rayleigh damping coefficients are function of the model's depth, this variation in depth also clarified how Rayleigh damping affects the model's results. However, results displayed in figure () show an irrelevant change in results. On the other hand, another sensitivity analysis was performed in order to justify the width of the model illustrated the effect of changing the model's width. Results had shown that the alteration of the model's width has a trivial effect on the results therefore an average width of 100m was used to compromise between calculation time and accuracy. This is seen in Figure 16. But a research item conducted by Rayhani and Naggar (2008) concluded after conducting comprehensive numerical modelling and centrifuge model tests, that the horizontal distance of the soil lateral boundaries should be at least five times the width of the structure to consequently avoid reflection of outward propagating waves back into the model. In the same study, they came to a conclusion that most amplification occurs within the first 30 meters of the soil profile therefore a maximum bedrock depth of 30 meters is recommended in numerical models -this comes in agreement with most of modern seismic codes (e.g., ATC-40 1996, BSSC 2003). As a

result, this justified assumption was adopted in this research item which consequently led to the choice of model depth of 30 meters and model width of 150m.

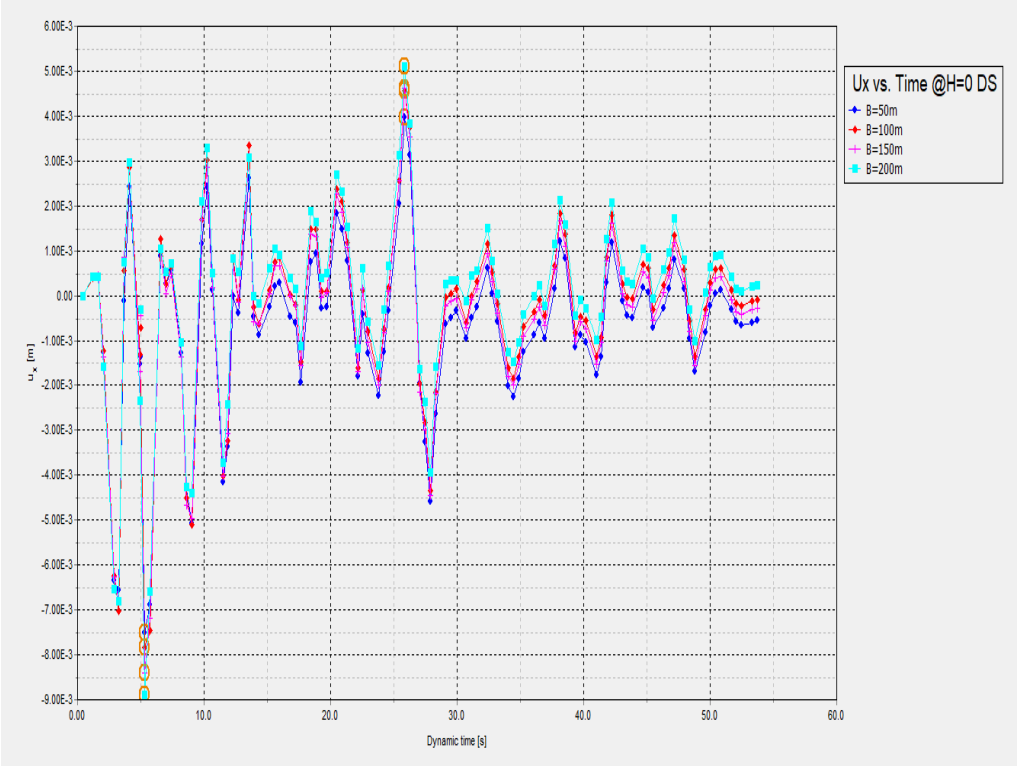

Figure 17 Horizontal displacement Ux vs. Dynamic time at H=0m, compared at different model widths

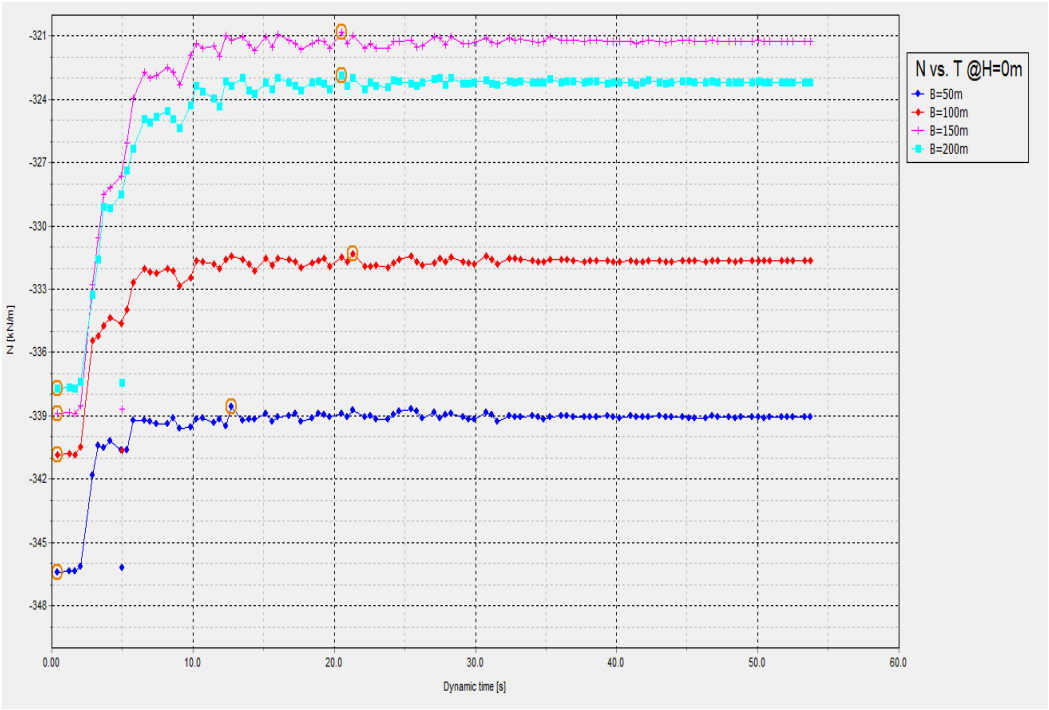

Figure 18 Axial force N vs. Dynamic time at H=0m, compared at different model widths

3.4 Soil constitutive model

HS-Small (Hardening Soil-Small strain) soil constitutive model, which is used in this research, was developed to cope with the high stiffness behavior the soil materials have when subjected to very small strains like earthquake vibrations. Brinkgreve, Kappert, and Bonnier (2007) explained in their paper the hardening soil constitutive model in Plaxis. This model is a non-linear model which assumes a hyperbolic relationship between stress and strain, and it adopts isotropic hardening. This model also includes two yielding surfaces to consequently differentiate between shear and isotropic loadings. Its formulation comes from modulus reduction curves where the shear modulus G is plotted against shear strain γ in a logarithmic function. These plots show the trend for points ranging from very small strains to large strains. In the HS-Small model, this curve is characterized by two parameters: the small-strain shear modulus G_0, and the shear

strain at which the secant shear modulus has reduced to 0.7 times G_0, $\gamma_{0.7}$. Moreover, this is the only model that accounts for hysteretic damping. The HS-Small model shows the typical hysteretic behavior of soil when subjected to small strains. Hysteretic damping is represented by a damping ratio ξ. This damping ratio represents the total accumulated dissipated energy in a complete load cycle and is a function of the small-strain shear modulus G_0 and the shear strain $\gamma_{0.7}$.

3.5 Soil Data

(Brinkgreve, Engin, & Engin, 2010) derived empirical equations that can be used to calculate the parameters associated with sand soil. Note that the use of these equations is limited to drained soil conditions. The equations are stated as followed:

$\boldsymbol{\gamma_D}$= 15+4.0RD/100 [Kn/m^3]

$\boldsymbol{\gamma_{sat}}$= 19+1.6RD/100 [Kn/$m^3$]

$\boldsymbol{E_{50}^{ref}}$= 60000RD/100 [Kn/$m^2$]

$\boldsymbol{E_{oed}^{ref}}$= 60000RD/100 [Kn/$m^2$]

$\boldsymbol{E_{ur}^{ref}}$= 180000RD/100 [Kn/$m^2$]

$\boldsymbol{G_0^{ref}}$ = 60000+68000RD/100 [Kn/m^2]

m= 0.7-RD/320 [-]

$\boldsymbol{\gamma_{0.7}}$= (2-RD/100).$10^{-4}$ [-]

Ψ'= -2+12.5RD/100 [º]

Φ'= 28+12.5RD/100 [º]

$\boldsymbol{R_f}$= 1-RD/800 [-]

These equations were consequently used to calculate the parameters for dense and loose sands which are relevant to this research paper and are displayed in Table 2.

Table 2 Soil Parameters

Soil Parameters				
Parameter	**Symbol**	**Dense Sand**	**Loose Sand**	**Unit**
Dry unit weight	**γ_D**	20	16.5	kN/m^3
Relative density	**Rd**	90	35	%
Shear velocity	**Vs**	500	225	m/s
Poisson's ratio	**V_{ur}**	0.2	0.2	–
Reference pressure	**p^{ref}**	100	100	kN/m²
Triaxial compression stiffness	**E_{50}^{ref}**	54000	21000	kN/m²
Primary oedometer stiffness	**$Eoed^{ref}$**	54000	21000	kN/m²
Unloading/reloading stiffness	**E_{ur}^{ref}**	162000	63000	kN/m²
Shear strain at 0.7G_0	**$\gamma_{0.7}$**	$1.1x10^{-4}$	$1.65x10^{-4}$	–
Small strain stiffness	**G_0**	121200	83800	kN/m²
Dilatancy angle	**Ψ'**	9	3	°
Friction angle	**Φ'**	40	33	°
Rate of stress dependency	**m**	0.4	0.6	–
Failure ratio	**R_f**	0.9	0.95	–
Cohesion	**C'**	3	1	kN/m²
Rayleigh Coefficient	**α**	0.04909	0.3534	-
Rayleigh Coefficient	**β**	1.901E-3	2.546E-3	-

3.6 Soil damping

Damping in soil can be defined as the loss of energy within the vibrating soil elements during cyclic loading. When a system is subjected to dynamic loads, it experiences several types of damping which are material damping, radiation damping, Rayleigh damping as well as viscous damping which is due to pore pressure and thus is neglected in this research. Material damping is the dissipation of energy due to the yielding of soil elements and their hysteretic behavior, whereas radiation damping is the dissipation of energy due to the wave propagation within the soil medium. It is important to note that neither Rayleigh nor numerical damping are classified as material or radiation damping. This is because these two forms of damping do not physically exist in a system subjected to dynamic loads, but interestingly is required to successfully complete a numerical analysis. This section sheds light on the abovementioned phenomenon.

Based on Newton's Law, for any object subjected to seismic loading the equilibrium equation in the form of a matrix is:

$$\mathbf{M}\ddot{\boldsymbol{Y}}+\mathbf{C}\dot{\boldsymbol{Y}}+\mathbf{K}\boldsymbol{Y}=-\mathbf{M}\ddot{\boldsymbol{Y}}\boldsymbol{g}$$

Where M, C and K are the system mass, damping and stiffness matrices, respectively. Moreoever, Y¨g is the input ground motion acceleration applied at the base of the system, and Y is the relative displacement vector with respect to the base of the system. Regarding the damping "C" matrix in the equation above, material damping is considered by the soil's constitutive model which simulates soil hysteretic stress-strain response and radiation damping is included by developing the finite element difference of the semi-infinite half space. These abovementioned phenomena will further be explained in this section.

3.6.1 Hysteretic Damping:

Hysteretic damping is known as the internal damping caused by energy dissipation due to friction in soil elements. In the context of energy dissipation, (Tatsuoka, Iwasaki & Takagi, 1978a) explained that some of the elastic energy stored in soil elements is consumed for destroying edges and structures of soil grains or transformed into energy in the form of sound or heat. This type of damping is frequency independent, in phase with the velocity and proportional to the displacement of the system. Hysteretic damping in the HS-Small model can be explained as follows. Starting from the small-strain shear stiffness, the actual stiffness will decrease with the increase in shear strain. Upon load reversal, the stiffness will start from Go and will decrease again until the next load reversal. The dissipated energy in a load cycle from -Yc to +Yc and back to –Yc, is equivalent to the area of the closed hysteretic loop, which is shown in figure 16.

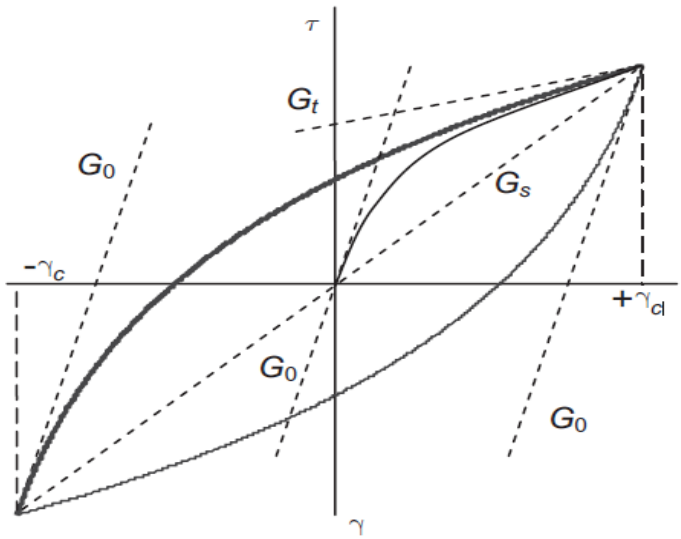

Figure 16 Hysteretic behavior in Small-strain model

Hysteretic damping is defined in terms of a damping ratio. This ratio is fundamentally defined as the ratio of the damping energy or dissipation energy in a soil element per cyclic loading W to the elastic energy or stored energy in the soil element per cyclic loading (W), better demonstrated in figure 17.

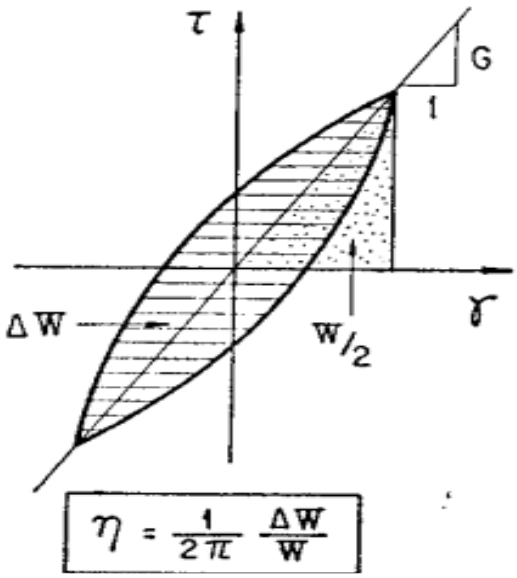

Figure 17 Definition of hysteretic damping ratio (Tatsuoka, Iwasaki, and Takagi 1978a)

As previously mentioned, (Brinkgreve, Kappert, & Bonnier, 2007) described hysteretic behavior in Plaxis where Hysteretic damping is characterized by two parameters: the small-strain shear modulus G_0 and the shear strain at which the secant shear modulus has reduced to 0.7 times G_0 ($\gamma_{0.7}$).

The local hysteretic damping ξ that is a function of the dissipated energy in a load cycle E_D and the energy stored at maximum strain Es, is defined as

$$\xi = \frac{4E_D}{4\pi Es}$$

Where

$$E_D = \frac{4G_0\gamma_{0.7}}{a}\left(2\gamma c - \frac{\gamma c}{1+\frac{\gamma_{0.7}}{a.\gamma c}} - \frac{2\gamma_{0.7}}{a}\ln\left(1+\frac{a.\gamma c}{\gamma_{0.7}}\right)\right)$$

$$E_s = \frac{1}{2}G_s\gamma c^2 = \frac{G_0.\gamma_{0.7}{}^2}{2+\frac{2a\gamma c}{\gamma_{0.7}}}$$

In this equation $a = 0.385\ and\ \gamma c =$ maximum strain due to cyclic loading

Figures **18** and **19** show the modulus reduction and damping curves associated with dense and loose sands, respectively.

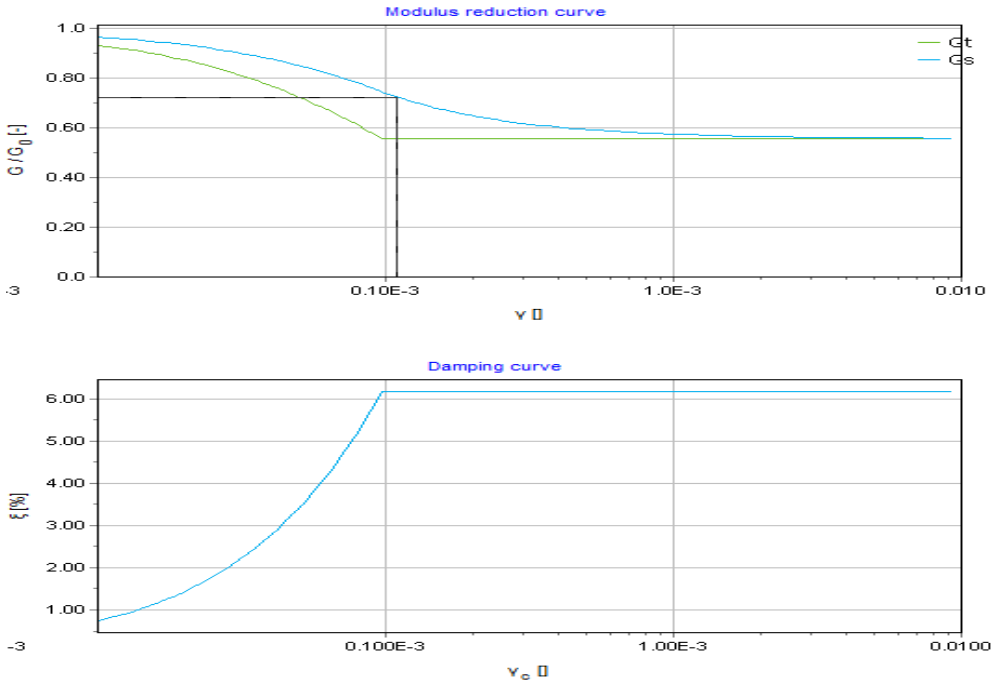

Figure 19 Modulus reduction and damping curves for dense sand

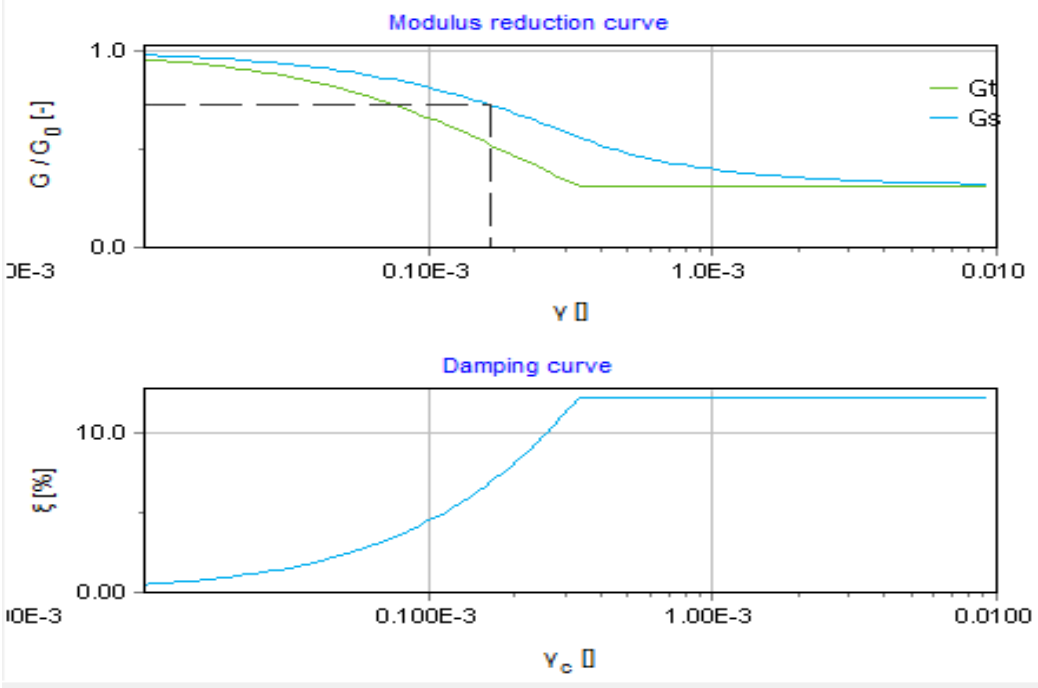

Figure 20 Modulus reduction and damping curves for loose sand

3.6.2 Radiation Damping:

Radiation damping is the damping within the soil-structure system caused by the generation and propagation of waves deviating from the foundation, which are due to the dynamic displacements of the foundation compared to the free-field displacements. Radiation damping is not part of the HS-Small model. It is a kind of geometric damping. In a 3D or 2D axisymmetric numerical model the attenuation of the wave amplitudes away from the source of vibration is automatically seen, where this is known as radiation damping. Therefore, radiation damping is not included in physical terms but is automatically functioning in Plaxis. Radiation damping is larger when the structure-to-soil stiffness ratio is larger.

3.6.3 Rayleigh damping:

Rayleigh damping is due to the energy dissipation in the P-waves and S-waves that propagate from the foundation level over a growing volume of the soil environment. This form of damping is represented by the Rayleigh coefficients alpha α, and beta β. These coefficients account for damping in both mass and stiffness matrices, respectively.

$$[C]= \alpha[M]+ \beta[K]$$

In the equation above, [C] is the damping matrix, [M] is the mass matrix, [K] is the stiffness matrix and α and β are the Rayleigh coefficients

In the formulation of Rayleigh damping in Plaxis, the damping matrix [C] is reduced to the form:

$$2\xi\omega = \alpha + \beta\omega^2$$

Where,

ξ =the damping ratio

ω= the soil circular natural frequency at n

α and β: the Rayleigh coefficients

These abovementioned equations are implemented in Plaxis. α and β are directly calculated whenever the double frequencies of the soil bed and the constant damping ratio are defined. These are derived as follows:

$$\omega_1= \frac{\pi Vs}{2D}$$

$$\omega_2= n\omega_1$$

$$n=\frac{\omega s}{\omega 1}$$

In these equations, Vs: shear wave velocity D: depth of the soil domain, ωs: fundamental frequency of the seismic input motion and n is an odd integer multiplier

greater than the ratio between the fundamental frequency of the seismic input motion ω_s and the first natural frequency of the soil ω_1 (Hudson, 1994)

3.6.4 Numerical damping:

To solve the equilibrium equation by numerical methods, it is necessary to introduce equations relating t¨, t˙, and t which correspond to displacement, velocity and acceleration, respectively. The Newmark family of implicit time integration schemes is generally implemented in geotechnical computer programs to provide the required equations. It must be taken into consideration that these equations are originally formulated based on Taylor series expansions for displacement, velocity, and acceleration by truncating the fourth time-derivative and higher form of the expansions. Hence, the numerical damping aspect of the model is like any other numerical modeling package. The procedure will further be discussed in the time-step section.

3.7 Interface elements

An interface is added to simulate the structure and the soil. An interface ensures that the structure and the soil are tied together: no relative displacement (slipping/gapping) is possible between structure and soil. By using an interface, node pairs are created between the structure and soil. Within a node pair, one node belongs to the structure while the other node belongs to the soil. The interaction between these two nodes of the pair consists of two elastic-perfectly plastic springs, one spring that is used to model the gap displacement and another to model slip displacement. Interface is characterized by Rinter in Plaxis. The level at which plastic slipping occurs is function directly to the strength properties and the Rinter value of the relevant material set. Changing the Rinter value

influences both the stiffness and the strength properties of the interface. The stiffness properties of the relevant material set are used to calculate the elastic shear and normal stiffness of the interface springs. This stiffness is chosen in a way that the program is numerically stable and elastic deformations are considered negligible. Moreover, the stiffness matrix for the interface elements is obtained using Newton cotes integration method where the position of Newton cotes stress points coincides with the node pairs. A Rinter value of 0.8-1.0 is recommended to simulate the interface between sand and concrete surfaces-dense sand and retaining/basement walls- while keeping its properties like the adjacent soil. In addition to reducing soil-structure interface strength, the interface also helps to avoid the occurrence of any non-physical peak stresses at plate ends. A Rinter of a value of 0.9m has been used in the modelling.

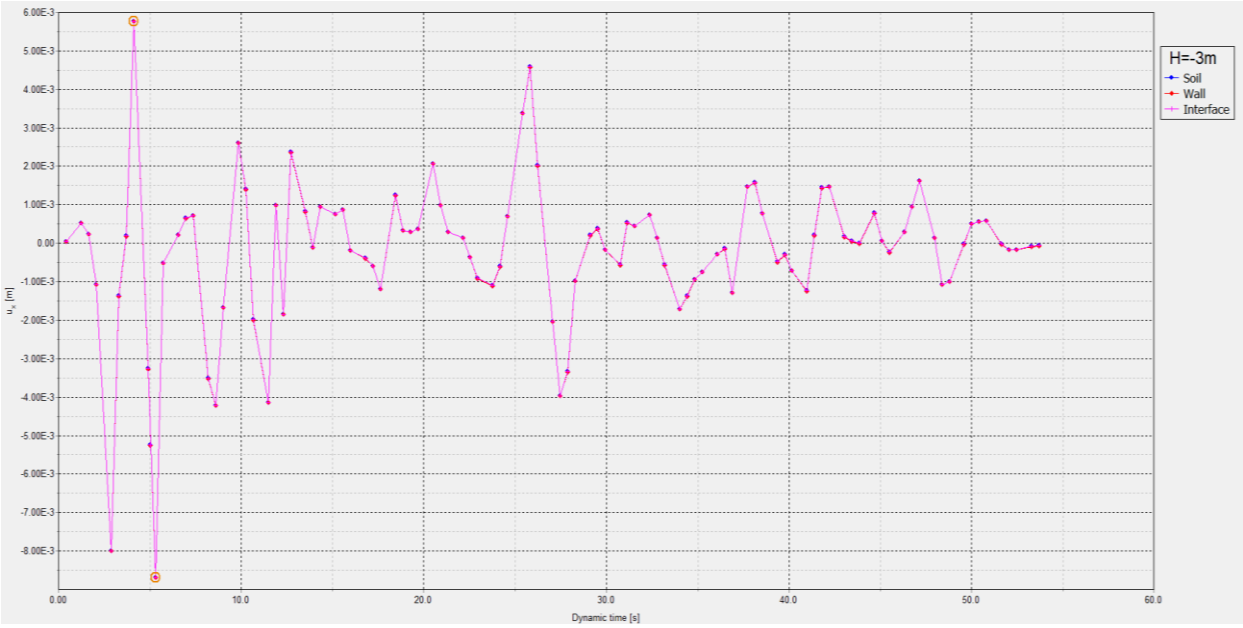

Figure 21 Horizontal displacement vs. time for soil, wall, and interface elements at depth of H=-3m

At an exact location, the soil element, interface element and wall element respond similarly which represents the interface's behavior.

3.8 Building Model

Plate elements are used to model the columns, slabs, walls and retaining walls while taking into account their respective strong axes and thicknesses. In figure 18, a detailed display of the structural elements found in each floor plan is presented. Plates are generally used to simulate the influence of walls, shells or linings extending in the z-direction. The material properties of plates are present in material data sets. The most important parameters are flexural rigidity (bending stiffness) EI and the axial stiffness EA, which have been calculated as shown in Table 3. Given these two parameters, an equivalent plate thickness d_{eq} can be calculated from the following equation:

$$deq=\sqrt{\frac{12EI}{EA}}$$

Given the values stated in table 3, the corresponding plate thicknesses for the building and basement plate elements are 0.3m and 0.4m, respectively.

Noting that the building is modelled as a two-dimensional frame structure, an equivalent load was estimated for each floor. Finally, the plate elements are modelled according to 5% damping Rayleigh coefficients.

Table 3 Material Properties of the Walls and Slabs (Plate Properties)

Parameter	Name	Building	Basement	Unit
Material Type	-	Elastic	Elastic	-
Isotropic	-	Yes	Yes	-
Axial Stiffness	EA1	900000	1200000	Kn/m
Bending Stiffness	EI	6750	16000	Knm^2/m
Plate Thickness	d	0.3	0.4	m
Weight	w	10	20	Kn/m/m
Poisson's ratio	v	0	0	-
Rayleigh α	-	0.232	0.232	-
Rayleigh β	-	8.00E-03	8.00E-03	-
Prevent Punching	-	No	No	-

Table 4 Material Properties of the Columns (Node-to-node anchor)

Parameter	Name	Column	Unit
Axial Stiffness	EA	2500000	Kn
Out-of-plane spacing	Lspacing	3	m

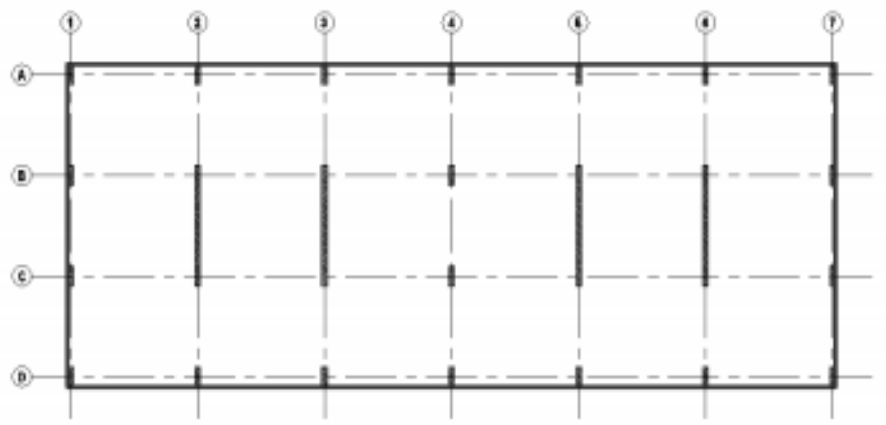

Figure 22 Typical building's floor plan

3.9 Applied Loads

3.9.1 Earthquake input signal

Loma Prieta is the input earthquake signal used in this research item. Data from the SMC-origin file is imported into Seismosignal software to extract the earthquake signal characteristics which are presented in Table 5. The acceleration time history which is extracted from seismosignal is translated into a Plaxis compatible format using Matlab. Knowing that drift might occur due to the integration of the accelerations and velocities, a drift correction is done. Drift (final displacement in the signal≠0) is further corrected by the application of a low frequency motion from the beginning of the calculation phase and by correcting the acceleration accordingly. Earthquake vibrations are simulated by a prescribed horizontal displacement applied at the base of the model- Bedrock. The same earthquake input was multiplied by 3 to resemble the effect of 3 times the Loma Prieto earthquake, this was done by tripling the dynamic multipliers.

Table 5 Earthquake signal's parameters

Parameter	Corrected Accelerogram	Unit
Max acceleration	0.1	g
Time of max acceleration	10.92	s
Max velocity	0.12606	cm/s
Time of max velocity	10.8	s
Sustained maximum acceleration	0.048	g
Sustained maximum velocity	0.04098	cm/s
Predominant frequency	2.63	hz
Predominant period	0.38	s
Number of effective cycles	1.7311	-
Maximum frequency	25	hz

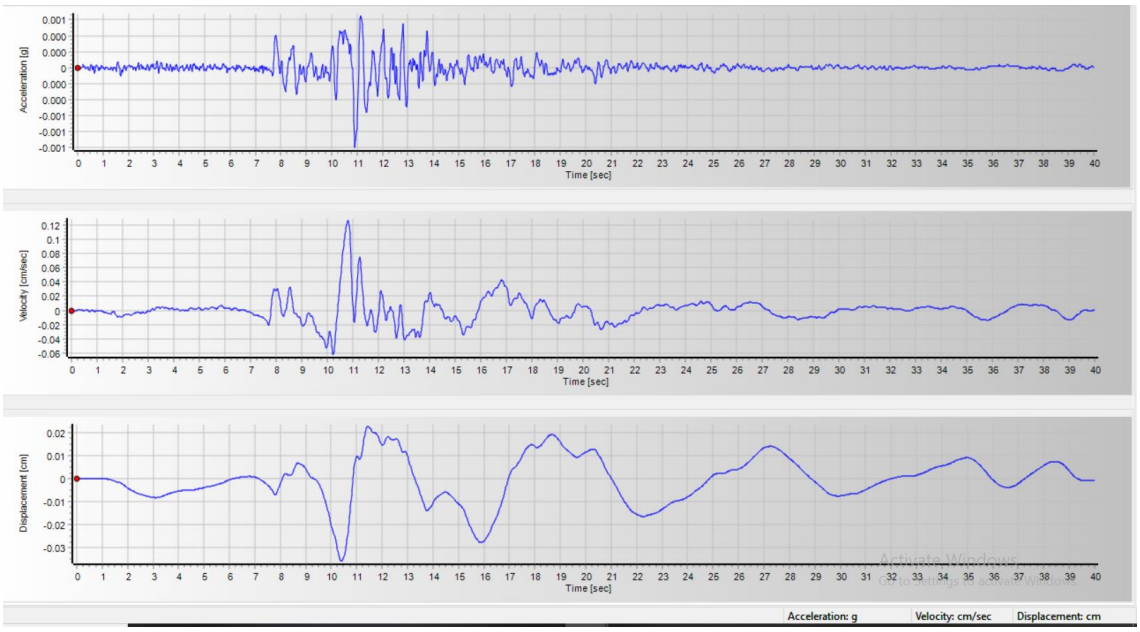

Figure 23 Acceleration, velocity, and displacement time graphs for Loma Prieta Earthquake

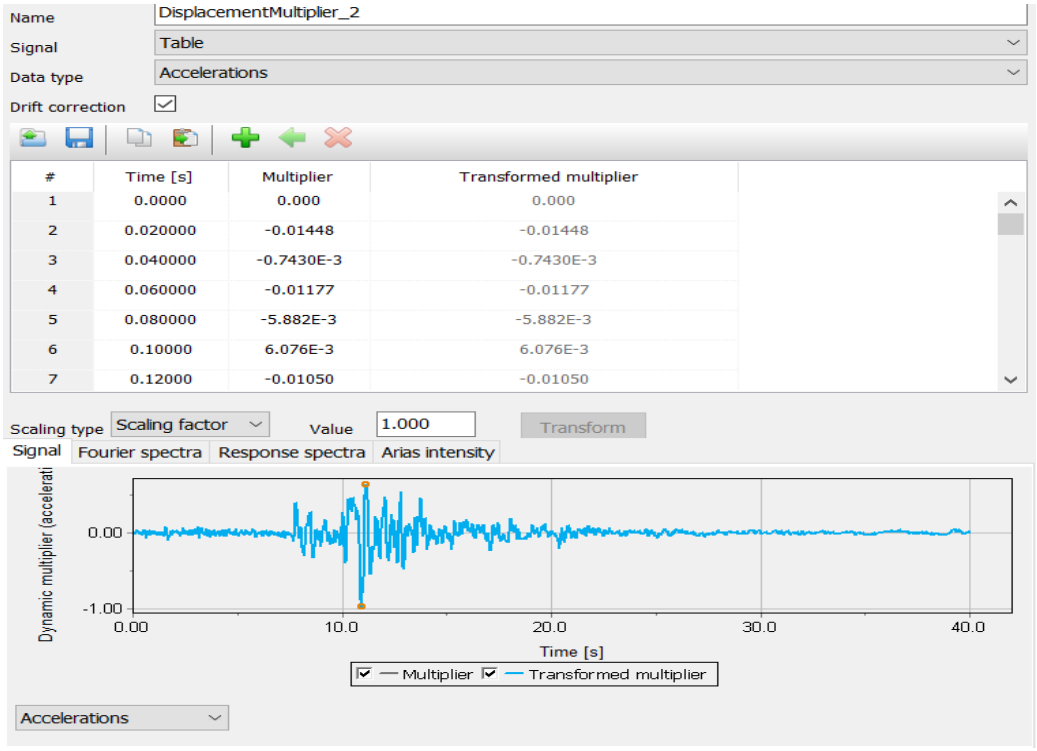

Figure 24 Dynamic multipliers for Loma Prieta Earthquake

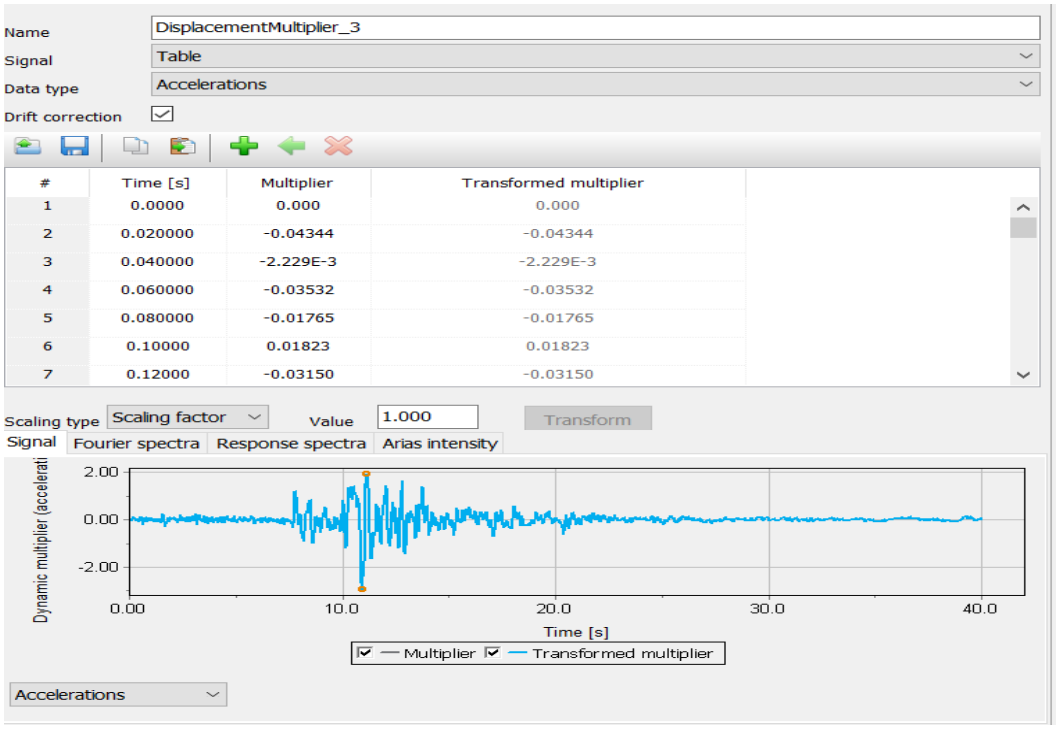

Figure 25 Dynamic Multipliers for Loma Prieta x3 Earthquake

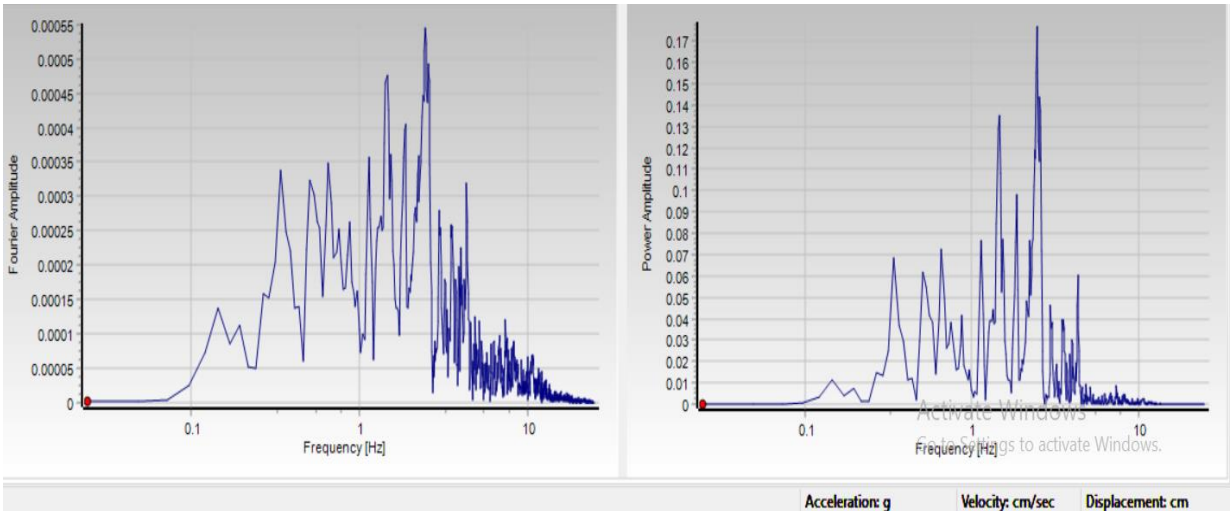

Figure 26 Fourier amplitude and power spectrums of Loma Prieta Earthquake

3.9.2 Building

The weight of the building is calculated roughly by estimating the approximate dead load of each floor. Only dead and super imposed dead loads are considered in the analysis to account for service loading combinations. Two values for the service loadings are used: floors from 0-15 are subjected to 5kN/m whereas the basement floors -1 to -3 are subjected to 6kN/m, both the vertical downward direction.

3.10 Dynamic boundary conditions

Different boundary conditions than the standard fixities are required in order to represent the far-field behavior of the soil medium. The reality is characterized by an infinite domain which has to be reduced to a finite domain when creating a geometry model. Appropriate boundary conditions can simulate the far-field behavior by absorbing the increment of stresses caused by dynamic loading and by avoiding spurious wave reflections inside the soil body. As such, the horizontal boundaries (Xmin,Xmax) are set as free-field boundaries (Figure 27 explains a free-field boundary behavior) . These

boundaries are made up of load history and viscous boundaries. The load history is the load coming from the free-field motion at the source's particular level which, in this case is the Bedrock. A viscous boundary is made up of viscous dampers of Lysmer type. These dampers provide a resistant force acting in the normal and tangential directions at the boundary that is proportional to the velocity in the material that is adjacent to the boundary. The relaxation coefficients C1 and C2 are used to improve the absorption of waves on these boundaries. C1 corrects the dissipation in the normal direction whereas C2 does it for the tangential direction. The standard values that have been used in this thesis are C1=1and C2=1, which accounts for pressure waves that only strike the boundary perpendicular, relaxation is redundant (C1= C2=1).

The normal and shear stress components absorbed by the viscous dampers (for the case of x direction) are formulated as follow.

$$\sigma n = -\mathrm{C1}\ \rho\ Vp\ \dot{ux}$$

$$\tau = -\mathrm{C2}\ \rho\ Vs\ \dot{uy}$$

Where ρ is the density of the material and Vp and Vs are the pressure and the shear wave velocities, respectively.

In addition, the vertical boundary (Ymax) is set as compliant base. The compliant base is a combination of a line prescribed displacement and a viscous boundary. However, the vertical boundary (Ymin) is set as none, which simulates standard fixities at the base making it a reflective base. This combination of boundaries allows for an earthquake motion input while still absorbing the incoming waves.

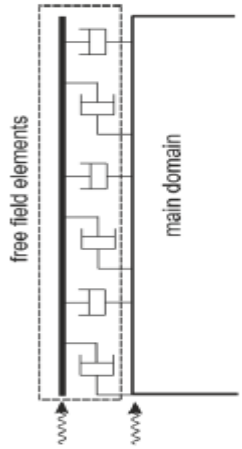

Figure 27 Free Field Elements

3.11 Mesh:

When the mode geometry is fully defined, the geometry has to be divided into finite elements in order to perform finite element calculations. A composition of finite elements is called a mesh. Plaxis 2D generates the mesh based on a robust triangulation procedure. The mesh should be sufficiently fine to assist in obtaining accurate results while on the other hand should be compensated with long calculation times. The element mesh size in models subjected to earthquake vibrations must be less than or equal to one-eighth of the minimum wavelength of the input signal, which depends on the shear wave velocity of the soil and the maximum frequency component of the input wave (Lysmer & Kuhlemeyer, 1969)

$$\text{Element size} \leq \frac{1}{8} Fmax$$

The average element size is calculated from the outer geometry dimensions (x_{min}, x_{max}, y_{min}, y_{max}) and is defined by the following formula.

$$Ie=\frac{re}{20}\cdot\sqrt{(xmax-xmin)2+(ymax-ymin)2+(zmax-zmin)2}$$

The finer the mesh, the higher is the computation time and the memory consumption. Therefore, a convergence study was performed for the case studies in this thesis, to optimize the mesh. However, a mesh size of less than 0.2m is used.

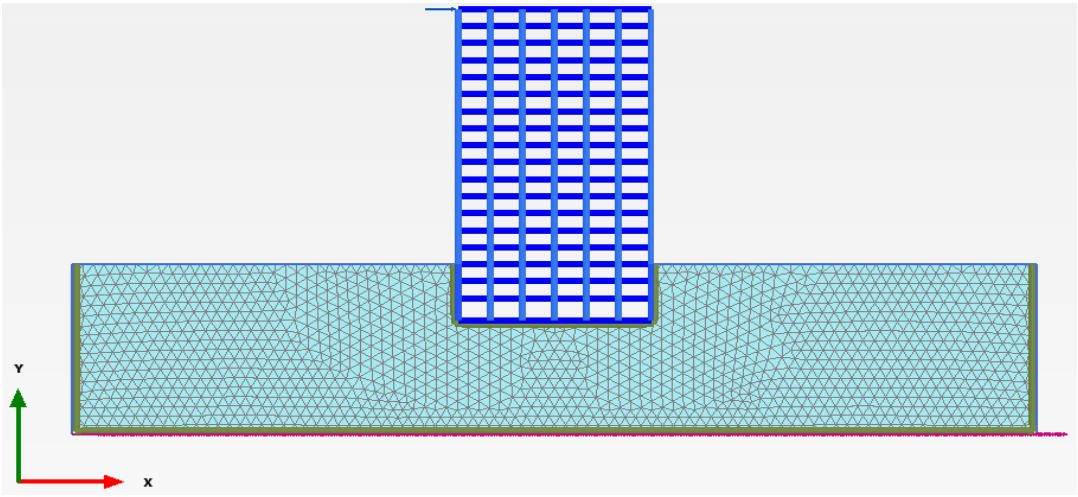

Figure 28 Numerical model with fine mesh

3.12 Phases of Construction:

The analysis in PLAXIS for the all the models is carried out in three stages:

1. Initial phase → Direct generation of initial effective stresses, pore pressures and state parameters.

2. Building phase → Installation stage of the building on sand.

3. Earthquake phase → Simulation of the building subjected to earthquake input signal.

3.12.1 Initial phase: Initial stress generation

The initial stresses in a soil body are influenced by the weight of the material and the history of its formation. This stress state is usually characterized by an initial vertical effective stress (σ'_{vo}). The initial horizontal effective stress $\sigma'_{h,o}$ is related to $\sigma'_{v,o}$ by the coefficient of lateral earth pressure K_0

$$\sigma'_{h,o} = K_o.\sigma'_{v,o}$$

$$K_o = K_o^{nc} OCR - \frac{vur}{1-vur}(OCR-1) + \frac{K_o^{nc} - \frac{vur}{1-vur} pop}{|\sigma yyo|}$$

These initial stresses are generated by means of the K_o procedure, available in Plaxis. When this calculation type is adopted, Plaxis generates vertical stresses that are in equilibrium with the self-weight of the soil. Horizontal stresses, on the other hand, are calculated from the specified value of K_0. At the end of the K_0 procedure, the entire weight of the soil is activated.

3.12.2 Building Phase: Plastic Calculation type

A Plastic calculation is used to carry out an elastic-plastic deformation analysis where it is not necessary to take the change of pore pressure with time into consideration. Here, the stiffness matrix is based on the original undeformed geometry of the model.

3.12.3 Earthquake phase: Dynamic Calculation type

The dynamic option should be selected as the calculation type when it is necessary to consider stress waves and vibrations in the soil medium. In Plaxis, the dynamic calculation is based on the equation that comes as the base for the time-dependent movement of a volume under the influence of a dynamic load, which is given by;

$$M\ddot{u} + C\dot{u} + Ku = F$$

In which M is the lumped mass matrix, u is the displacement vector, C is the damping matrix, K is the stiffness matrix and F is the load vector.

- The M matrix is implemented as a lumped matrix which includes the mass of the materials –soil, water or any constructions.
- The C matrix is formulated as a function of the mass (M) and the stiffness matrices (K) if the Rayleigh damping parameters are provided by the user.

- The K matrix accounts for the complete stiffness of the system. In case of undrained analysis, the bulk stiffness of the groundwater is then added to this matrix.

3.13 Time Steps and Time integration

The dynamic equations of motion are integrated based on time stepping schemes. These are characterized by several factors: the accuracy of calculation features, numerical damping and stability. In other words, these depend on the Newmark damping coefficients, the number of steps and sub steps, and the mass matrix. Within its embedded code, Plaxis ensures that a wave doesn't cross more than one element per time step. The critical time step is first estimated according to element size and material stiffness then the time step is adjusted based on the data points that are defined as dynamic multipliers. In addition, the time integration is carried out using Newmark's implicit time integration scheme. With this method, the displacement and the velocity at .the point at the time t+Δt are expressed as follow

$$u^{t+\Delta t} = u^{t} + \dot{u}^{t}\Delta t + \left(\left(\frac{1}{2} - \alpha\right)\ddot{u}^{t} + \alpha\ddot{u}^{t+\Delta t}\right)\Delta t^{2}$$

$$\dot{u}^{t+\Delta t} = \dot{u}^{t} + \left((1-\beta)\ddot{u}^{t} + \beta\ddot{u}^{t+\Delta t}\right)\Delta t$$

In the above equations, the variables β and γ are the numerical parameters that control both the stability of the method and the amount of numerical damping introduced into the system by this method. For a stable solution the following conditions must apply;

$$\beta \geq 0.5, \quad \geq \frac{1}{4}\left(\frac{1}{2} + \beta\right)2$$

For this thesis, default values of α=0.25 and β =0.50 are utilized which represents no numerical damping. This results in the generation of high frequency noises that often cause serious problems in computations by triggering instability of the computation

process, especially when the system has a large number of degrees-of-freedom and has a nonlinear material behavior is considered (Honda and Sawada, 2000).

3.14 Critical time step:

The critical time step in plaxis during a dynamic calculation is constant and is defined by

$$\Delta t = \frac{T}{m*n}$$

Where T is the time interval specific for every relevant phase, m is the number of additional steps required and n is the number of dynamic sub steps.

Multiplying the Additional step number (m) and the Dynamic sub steps number (n) results in obtaining the total number of steps that are to be used in the time discretization. It is also important to define a proper number of steps such that the dynamic signal used in dynamic loading is properly covered and simulated. In general, it is recommended to choose values for T, m and n in such a way that the dynamic sub step time interval Δt and the time interval used in the input signal are equal.

The critical time step ($\Delta t_{critical}$) can be defined by the following equation:

$$\Delta t critical = \frac{Ie}{\alpha\sqrt{\frac{E(1-v)}{\rho(1+v)(1-2v)}}\sqrt{1+\frac{B^4}{4S^2}}-\frac{B^2}{2S}\left[1+1-\frac{1-2v2S}{4\ B^2}\right]}$$

The terms B and S respectively denote the largest dimension and the surface area of a finite element. The factor α depends on the element type (for 15 node element $\alpha \approx 0.748$). The $\Delta t_{critical}$ is formulated in such a way that a wave during a single time step does not move a distance larger than the minimum dimension of an element. The user needs to choose T in such a way that $\Delta t \leq \Delta t_{critical.}$

Moreover, the maximum recommended time step depends on the maximum frequency and the coarseness or/and fineness of the finite element mesh. The equation used for a single element is:

$$\Delta_{tmax,recommended} = \frac{lmin}{Vs}$$

Where l_{min} is the minimum length between three nodes of an element and V_s is the shear wave velocity of an element.

The integration time step for the analysis was taken as 0.01s in order to accurately capture the input ground motion. Also, it is sufficiently small to capture the structure response, since it is considerably smaller than $\frac{1}{12}$ of the structure's period. Knowing that the fundamental period of the structure is 1.273s, calculated according to ASCE7-14 seismic requirements, the corresponding time step must be less than 0.706s accordingly, the time step used is 0.41sec.

CHAPTER 4

RESULTS

4.1 Introduction

In this chapter, the outcome of this research item is presented. The results are categorized to demonstrate different aspects of the inclusion of damping in soil-structure interaction analysis problems.

These aspects are presented as follow:

1- Significance of damping in both dense and loose sands

2- A comparison between the significance of damping under earthquake intensities.

3- A comparison between the effect of hysteretic and Rayleigh damping (each studied individually and combined)

4- The effect of damping inclusion on the lateral displacements of the retaining walls as well as the top of the building.

5- The effect of damping's inclusion on the structural base shear.

6- The effect of damping on the lateral pressures of the retaining walls.

Each of these is discussed in terms of graphs, numerical comparisons and a brief explanation of the graphs attached.

4.2 Results

4.2.1 Significance of Damping between Dense Sand and Loose Sand

Figure 29 and Figure 30 provide an illustration of the importance of including damping in the analysis of building encountering soil-structure interaction effects founded on loose sands, compared to those founded on dense sands. This importance is resembled in terms of graphs where the lateral displacements at ground level are plotted against the time of the earthquake (in Dense sands for figure 29 and loose sands for figure 30).

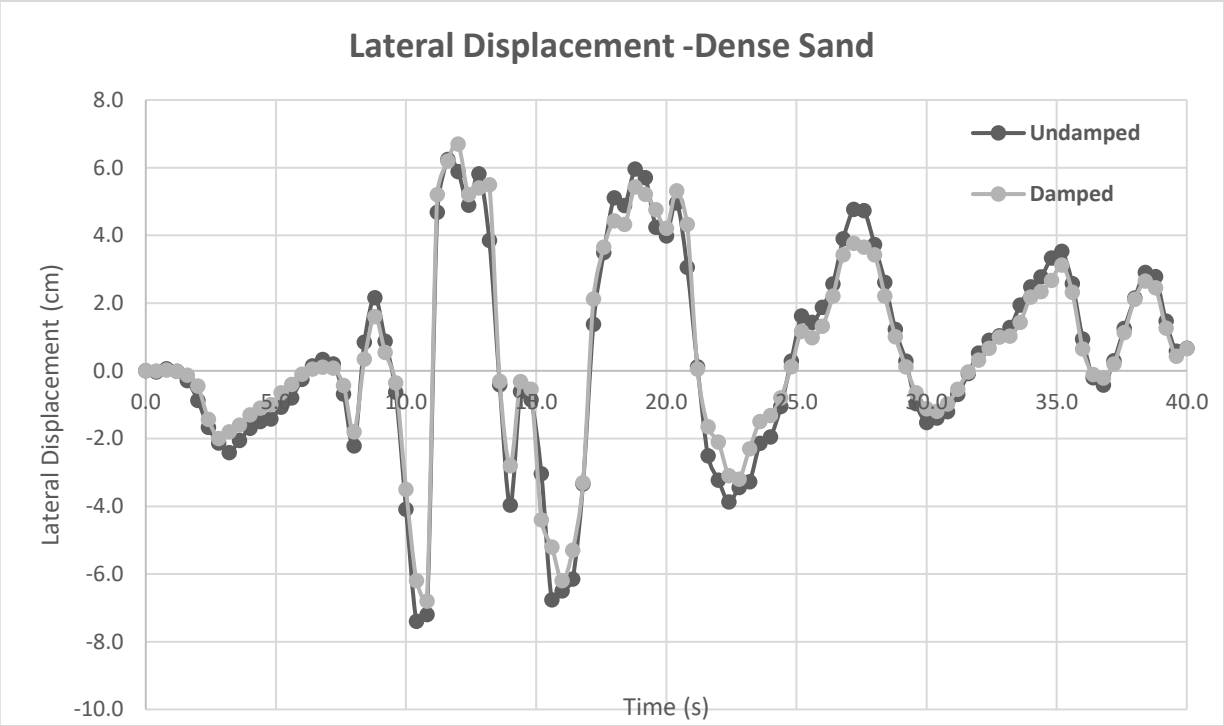

Figure 29 Lateral Displacements vs. Time (Dense Sand)

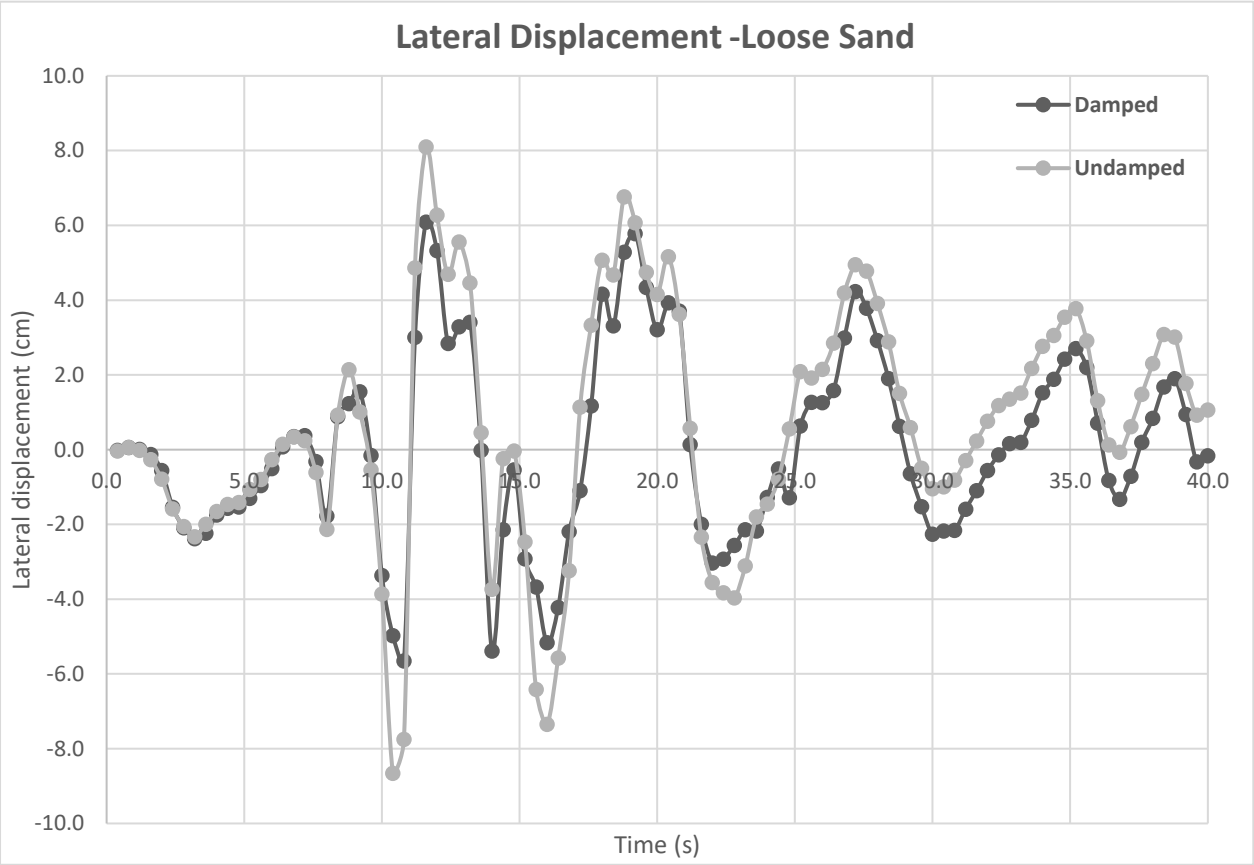

Figure 30 Lateral Displacements vs. Time (Loose Sand)

Both figures provide evidence for the significance of damping effects in loose sands compared to dense sand. This is justified by the fact that at time 10.4s the lateral displacement in dense sand's graphs was -7.4cm in the undamped model compared to -6.2cm in the damped model making a 16.2% reduction in lateral displacement. Moreover, within the same graph, the final permanent deformation was approximately 0.66cm for both the models. Whereas, in loose sands and at 10.4s the lateral displacement in the undamped model was -8.65cm compared to -4.97cm in the damped model making a 42.5% reduction in the lateral displacement. In addition, the permanent deformation in the undamped model was 1.04cm compared to 0.16cm in the damped model creating an approximate of 76% reduction.

4.2.2 Significance of Damping as a function of Earthquake Intensity

The effect of soil damping function of the earthquake input motion intensity can be explained in Figures 31 and 32. These graphs show the ground base shear at the same point of the same building that is subjected to Loma Prieto x1 Earthquake motion in a case and to the same motion by intensified by 3 times in another. The lateral displacements are plotted during the complete time of the Earthquake.

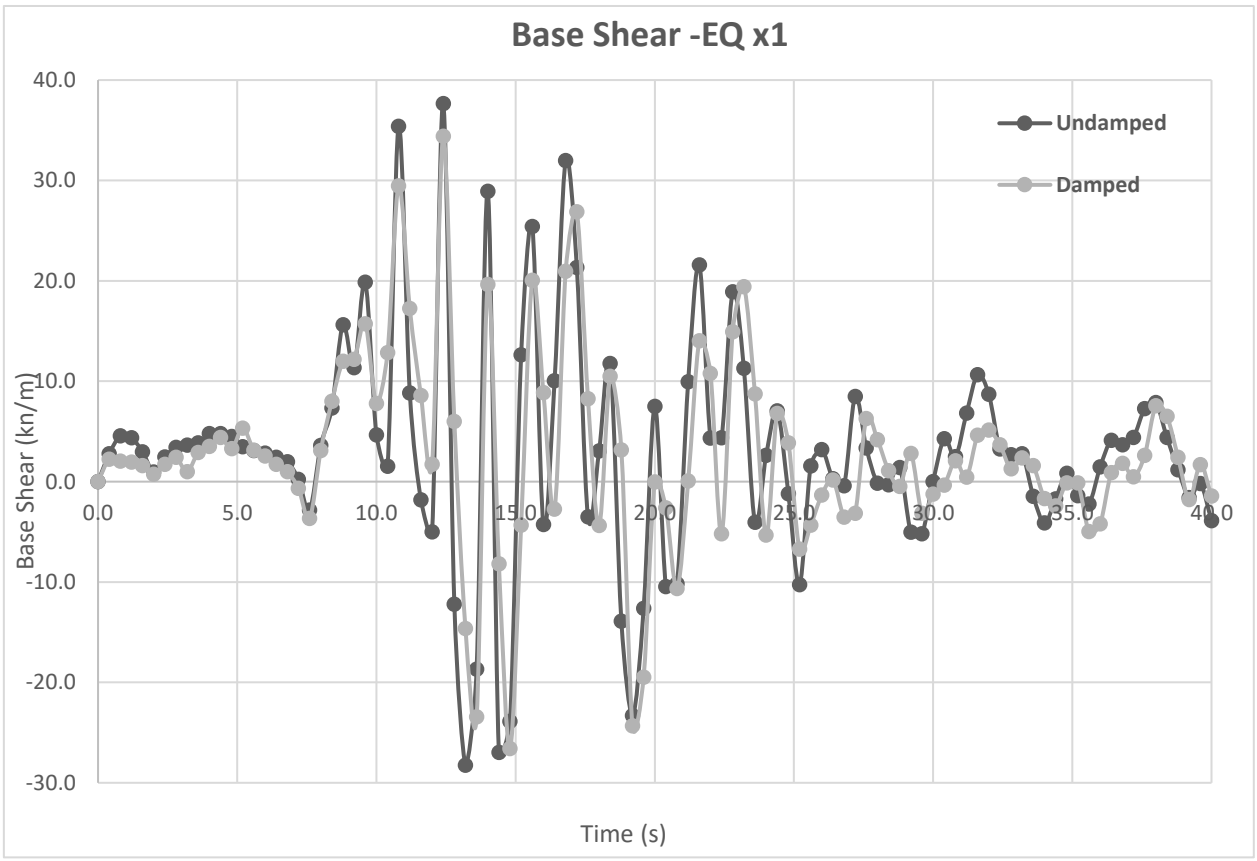

Figure 31 Base Shear vs. Time (Earthquake x1)

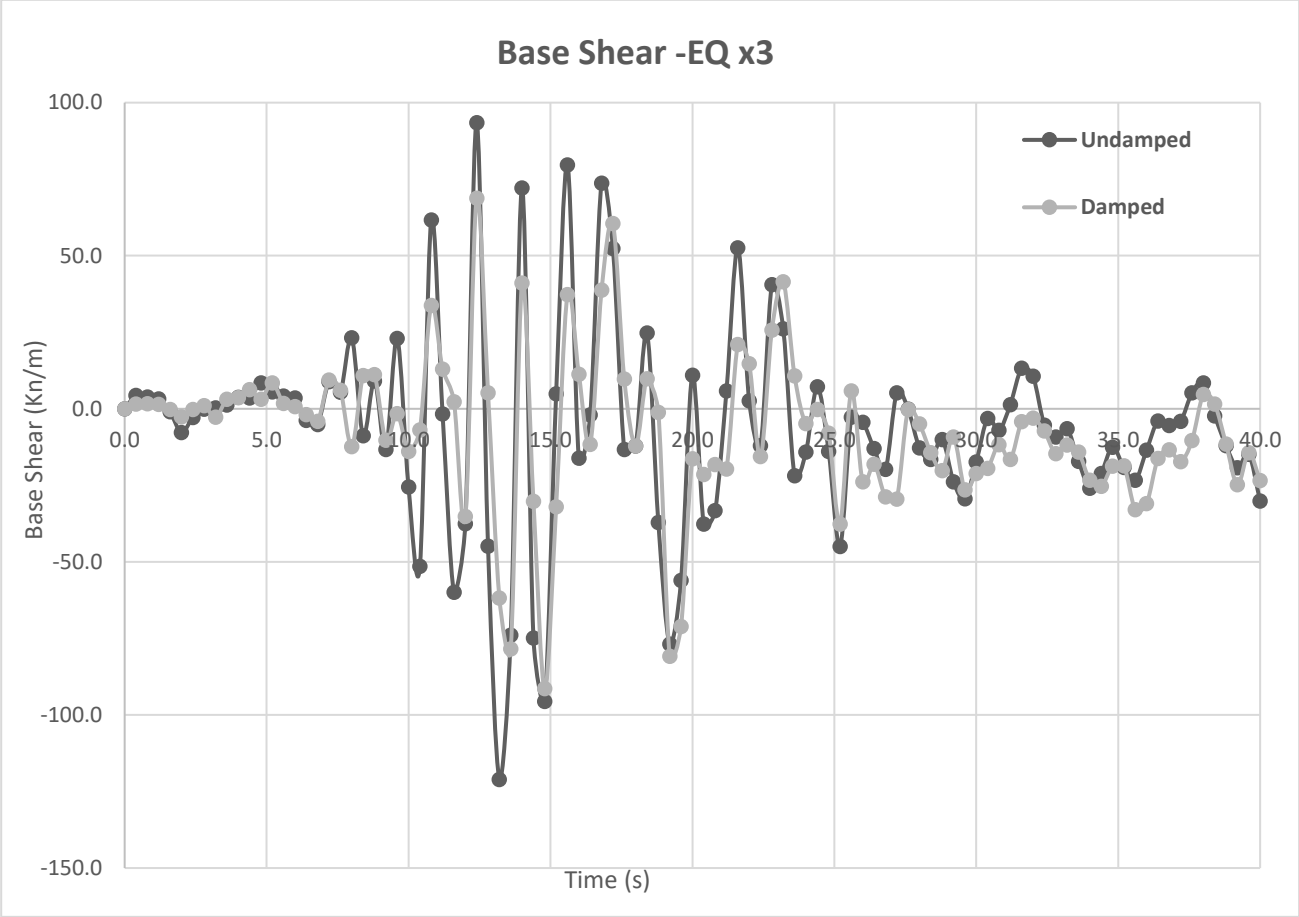

Figure 32 Base Shear vs. Time (Earthquake x3)

The abovementioned figures show that the effect of damping becomes more noticeable with respect to larger earthquake intensities. Looking at Figure 31 and the time of 13.2s the ground base shear is -28.25kn/m in the undamped model while -23.32kn/m in the undamped model making a reduction of 17.45%. on the other hand, and at the same time, results from figure 32 show an approximate 35% reduction in ground base shear.

4.2.3 Significance of Hysteretic Damping as compared to Rayleigh Damping

While studying the non-linear behavior of soils, hysteretic damping's effect is more significant compared to Rayleigh damping. This is observed in in Figure 33 in which the lateral displacement at the ground level is plotted against time for three conditions:

1- Considering soil hysteretic damping and Rayleigh damping

2- Considering Rayleigh damping only

3- Absence of both hysteretic and Rayleigh damping

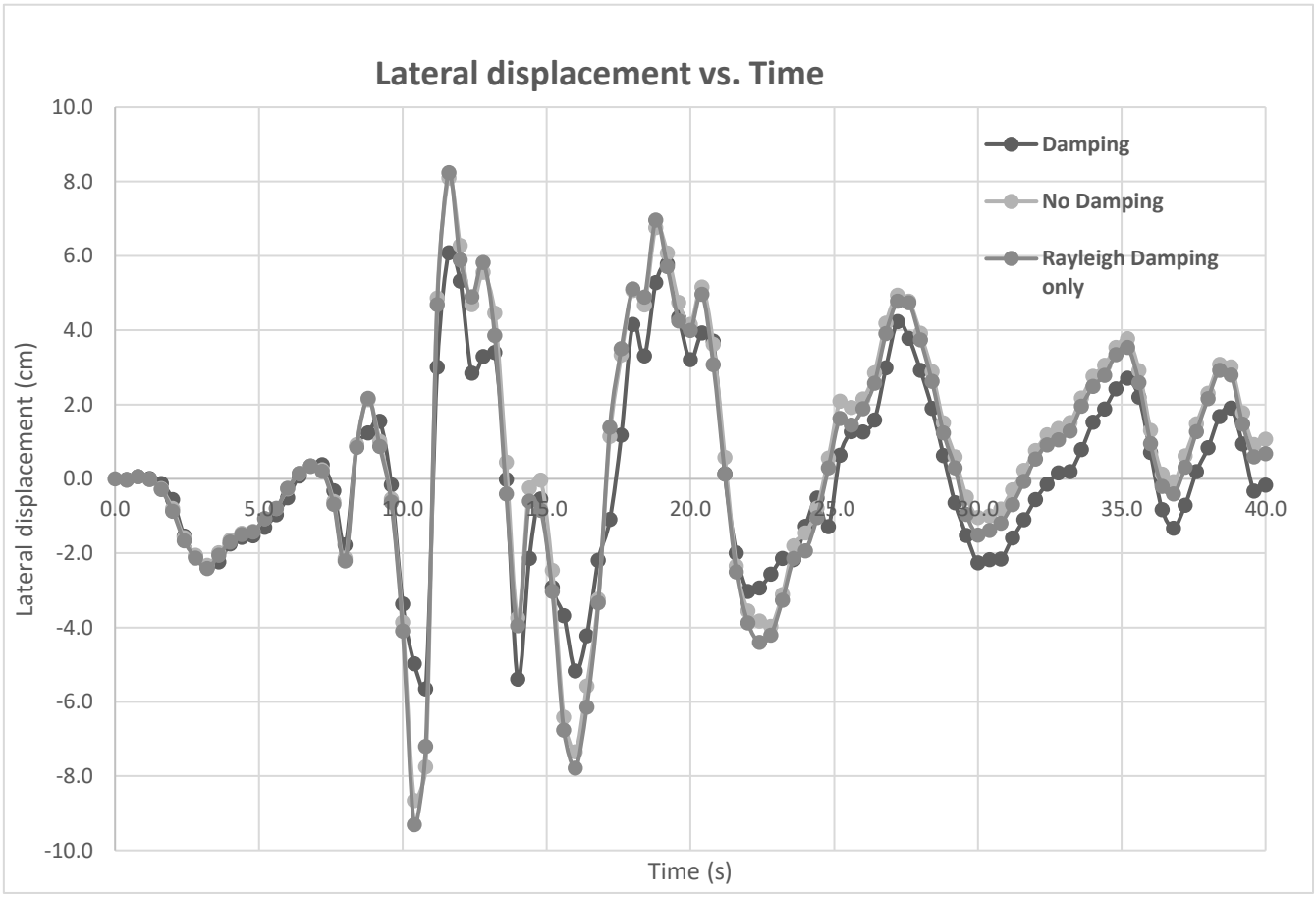

Figure 33 Effect Hysteretic, Rayleigh and both forms of damping combined on lateral displacements

Results from the graph show a very similar between the two models (Rayleigh damping only and the absence of the two sources of damping) while a noticeable decrease in the lateral displacement when considering the two sources of damping. This demonstrates the effect hysteretic damping in comparison to Rayleigh damping.

4.2.4 Effect of Damping on the Lateral Displacements

The inclusion of damping poses a decrease in lateral displacement in all cases of the analysis. This could be seen in Figure 35 and 36. However, figure 34 illustrates the lateral displacement of the building at different locations, this is to show the actual displacement of the entire building is simulated in Plaxis.

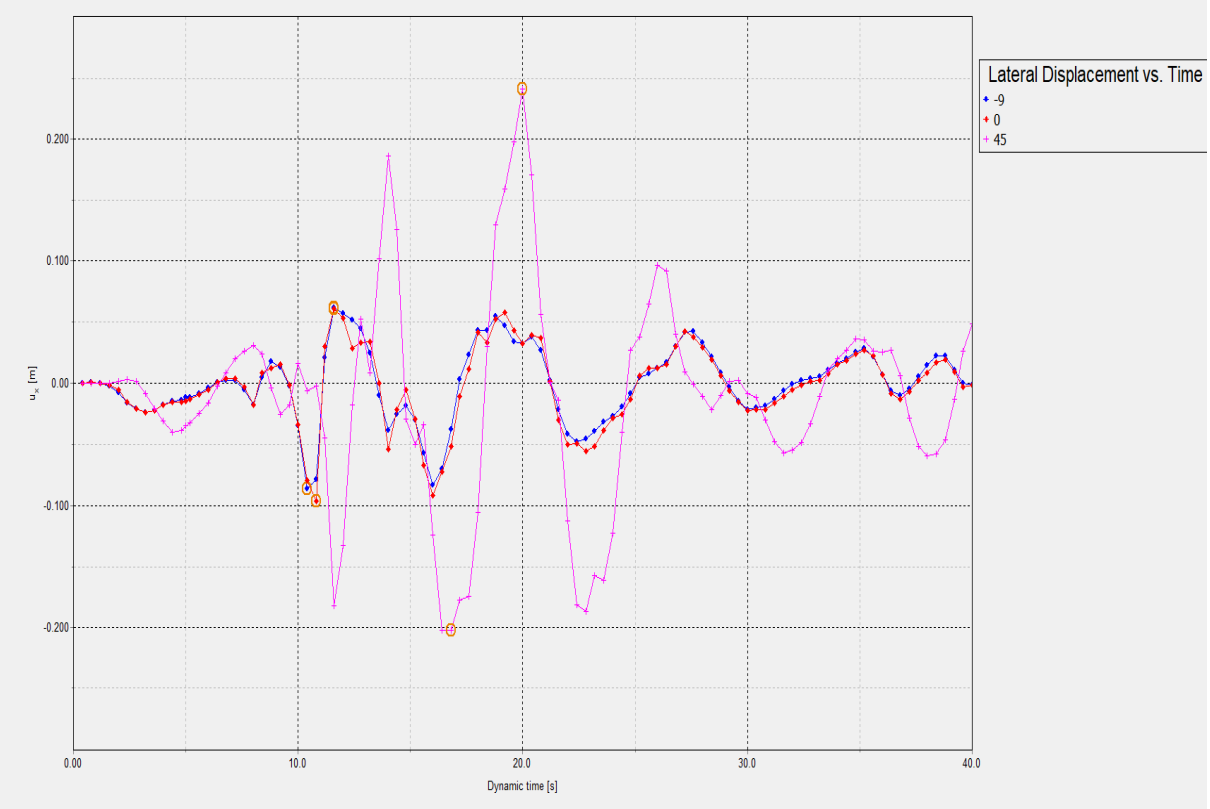

Figure 34 Lateral Displacements vs Time at (H=0m, H=45m and Z=-9m)

4.2.4.1. At the Ground Level (i.e H=0m)

Figure 35 illustrates the effect of damping on lateral displacements. The pattern shows that lateral displacement at the base of the building i.e H=0m decreased by 33.3% in the damped model compared to the undamped model.

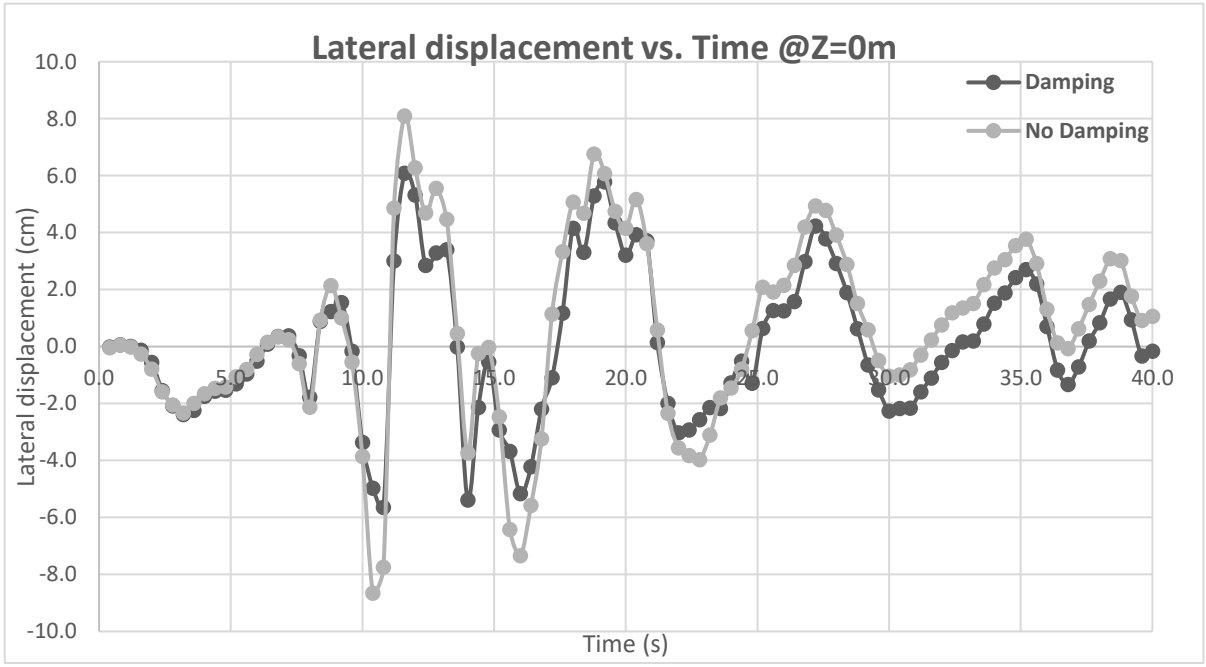

Figure 35 Lateral Displacement vs. Time (H=0m)

4.2.4.2 At the Roof Level (i.e H=45m)

Similar to the outcome of figure 36 the variation in horizontal displacement at the top of the building i.e 45m also shows that the displacement decreased by 62.5% in the damped model, at the end of the earthquake.

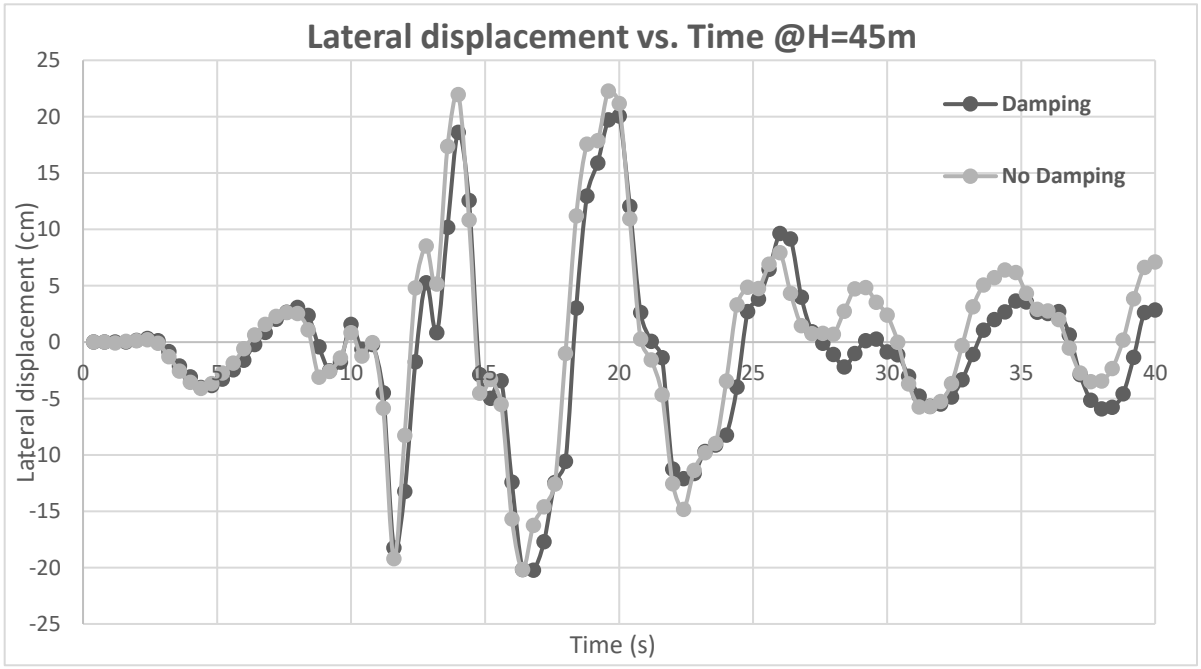

Figure 36 Lateral Displacement vs. Time (H=45m)

4.2.5 Effect of Damping on the structural base shear

Damping plays a significant role in reducing the base shear. This can be demonstrated in Figure 37 where the ground base shear induced during the Earthquake is plotted against the time of the earthquake.

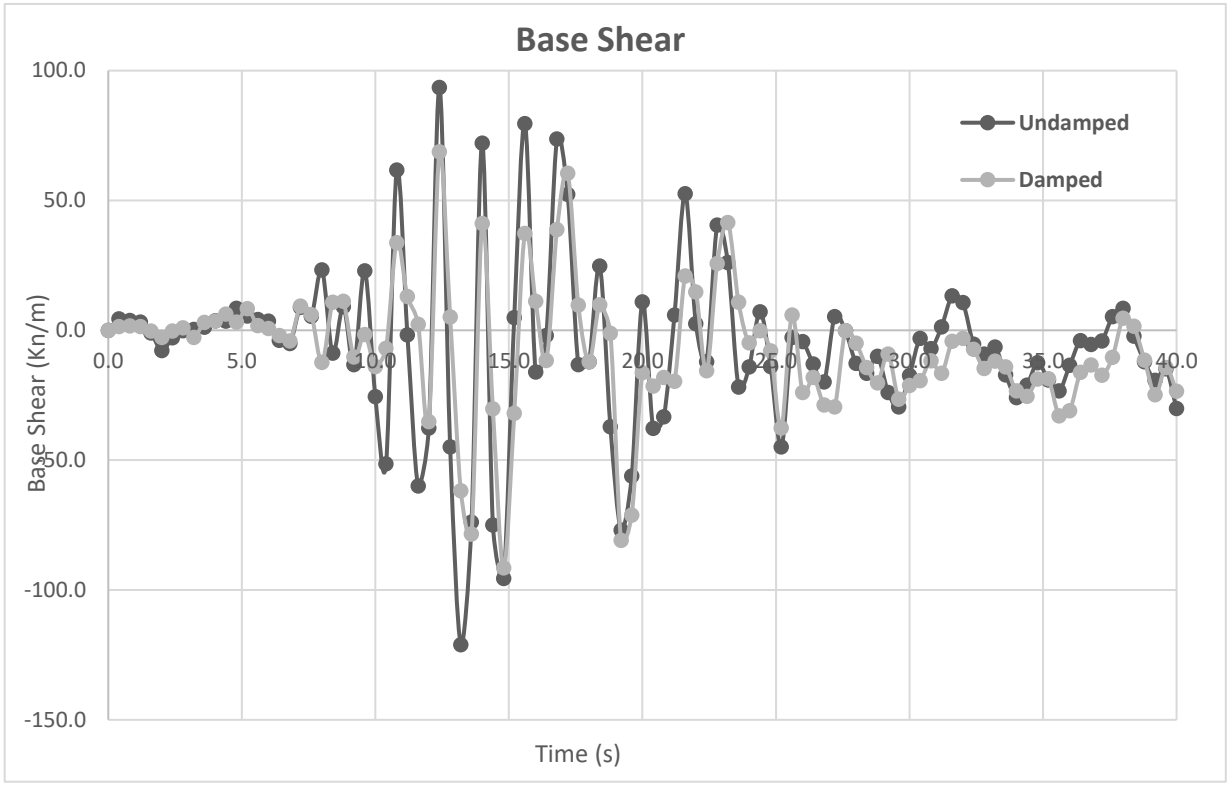

Figure 37 Base Shear vs. Time

Results from Figure 37 shows base shear decreased by 42.3% in the damped model compared to the undamped model. This base shear was compared to the manually calculated base shear where a 19.53% difference was observed between the manually calculated using the equivalent lateral force method which yielded a ground base shear of value 160.24Kn/m and the numerically obtained base shear.

4.2.6 Effect of Damping on lateral earth pressure

To accurately tackle the effect of damping on the lateral earth pressures along the retaining walls, a detailed study was found to be of need to complement the outcome of this research. In figure 38, which shows the numerical model at the end of the earthquake, provides a view of the position of the retaining walls (LW=Left Wall and RW=Right Wall)

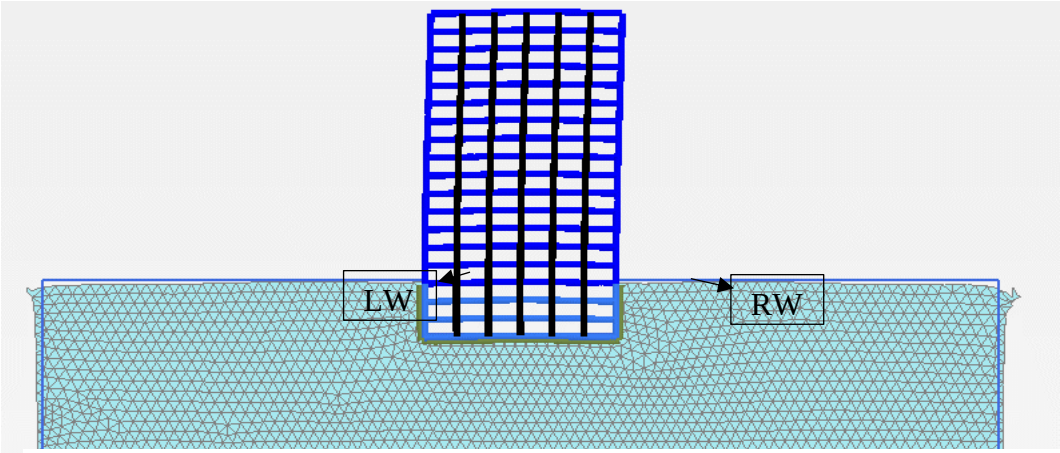

Figure 38 Position of the Retaining Walls

Moving accordingly, figures 39 and figure 40 present a visual for the movement of the retaining walls at the time at which the building experience maximum positive shear and at the time it is subjected to maximum negative shear. These displacements are shown in addition to the behavior (position) of the wall at the start of the earthquake and at its ending.

Noting that the presented graphs in this section are all obtained from the model in which the model is subjected to 3 times the Earthquake input motion.

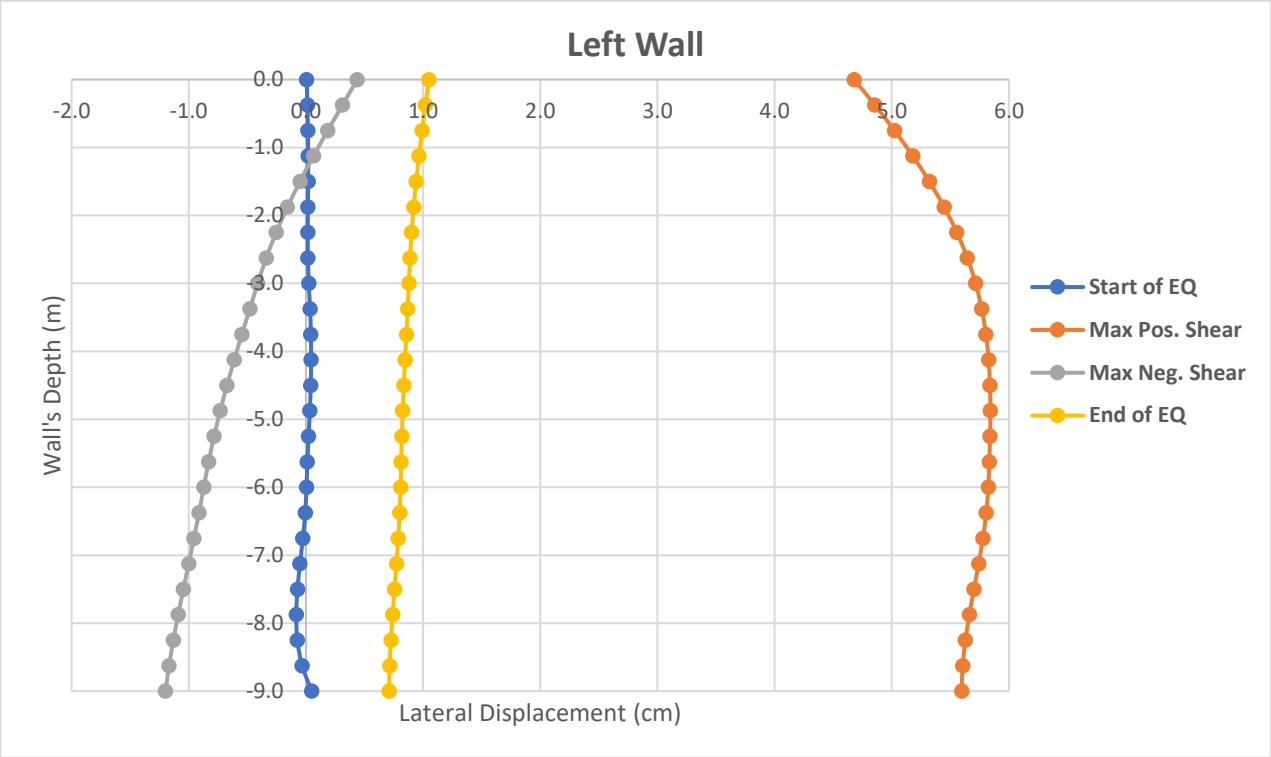

Figure 40 Lateral Displacement of the left wall at different times

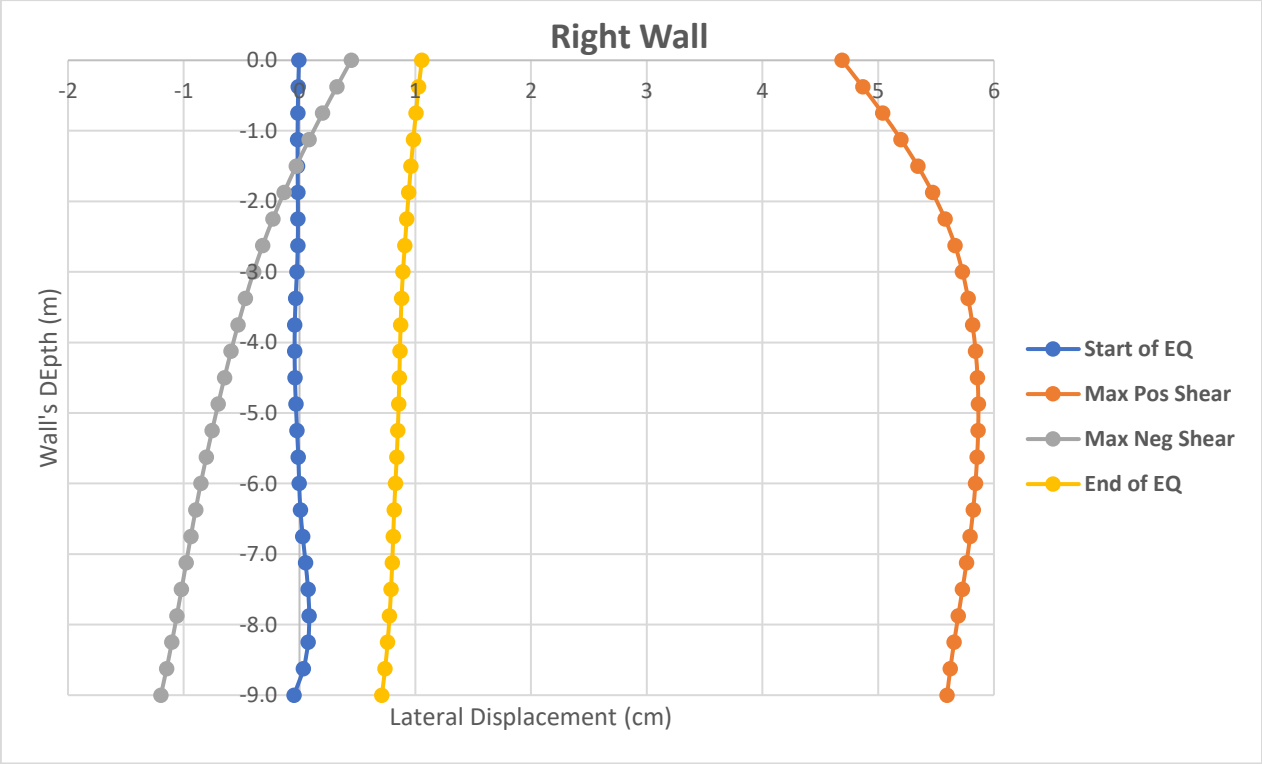

Figure 39 Lateral displacement of the left wall at different times

Taking into consideration that the two walls are moving simultaneously in a similar behavior, the corresponding normal stresses were obtained at the same timings.

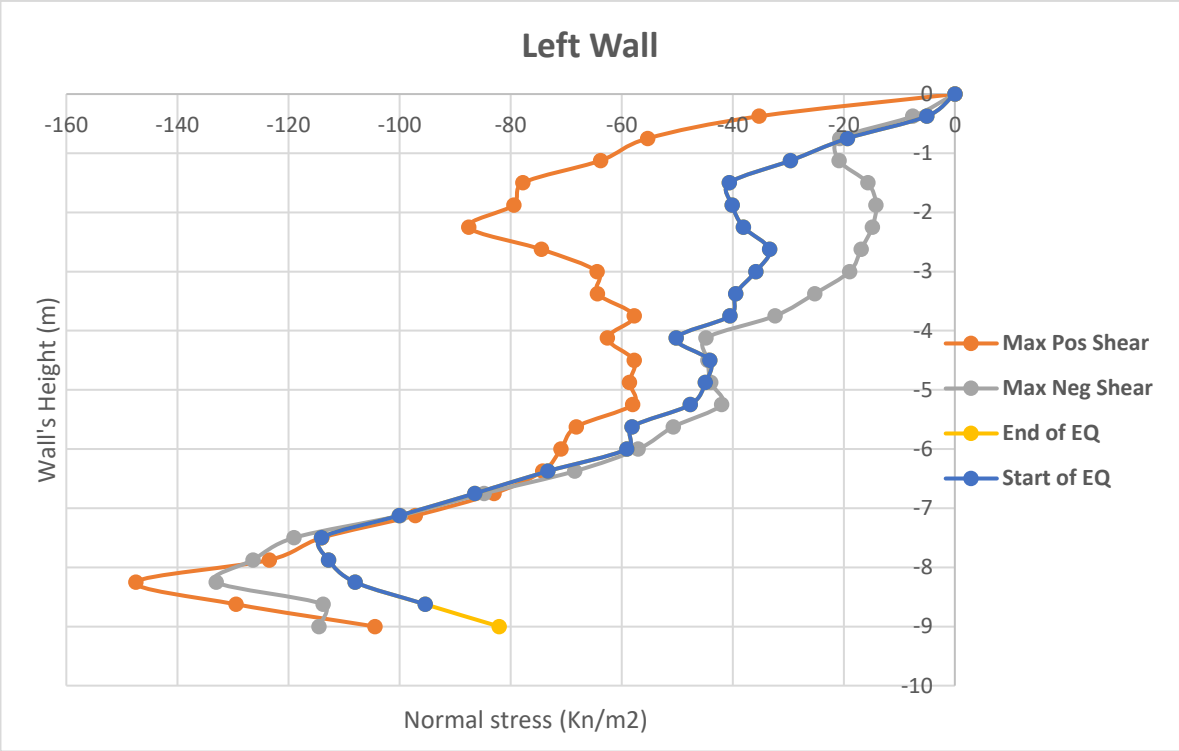

Figure 42 Normal stresses along the left wall at different times

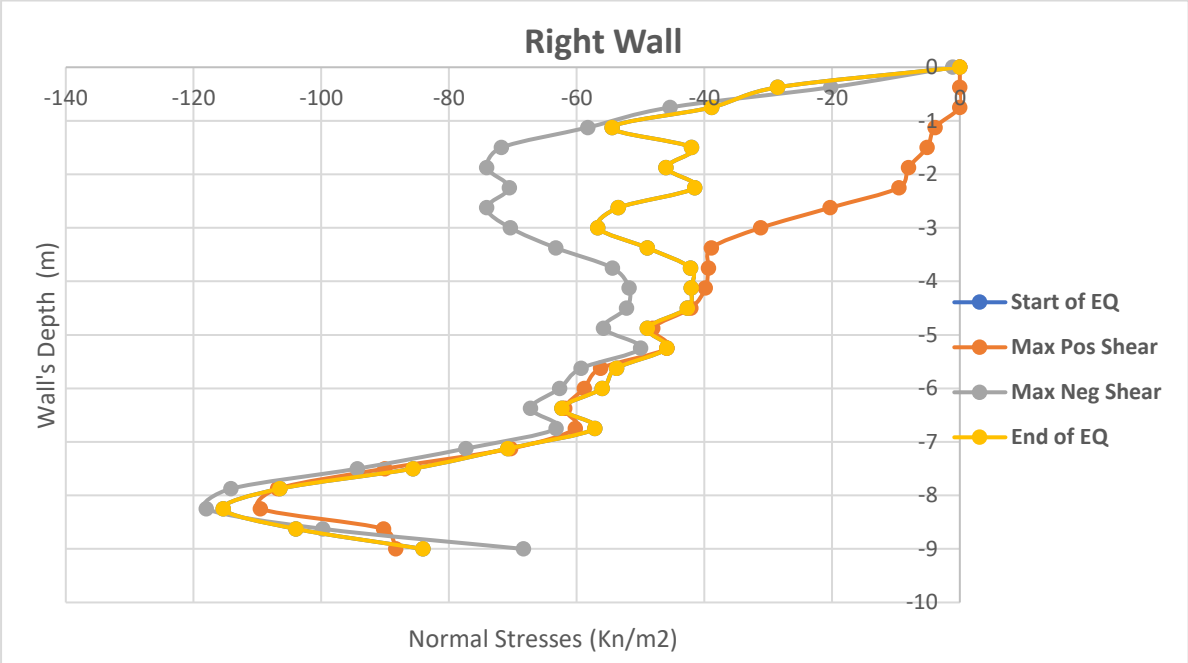

Figure 41 Normal Stresses along the Right wall at different times

Taking a close look on how the soil elements are responding to the earthquake motion can be seen in figure 42. Figure 42 provides a plot of the horizontal stresses along a section taking at a distance of 0.4cm from the wall and lies vertically along the depth of the wall, i.e 9m.

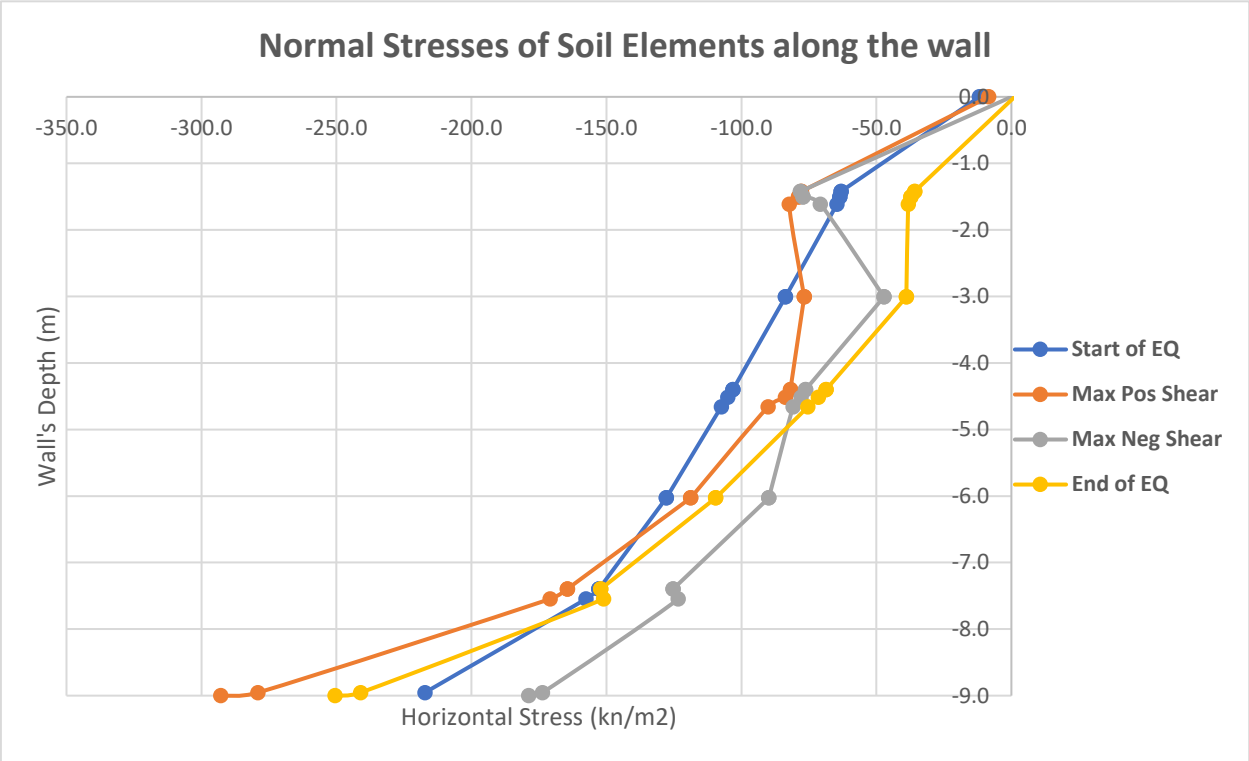

Figure 43 Horizontal stress of the soil elements (section taken along the depth of the wall)

Finally, the effect of damping on the lateral earth pressures can be illustrated in figures 44 and 45 that provide a comparison between the undamped and damped model's behavior in terms of the difference in the lateral earth pressures induced on the retaining wall in both the damped and undamped models (Figure 44) and the difference between the horizontal pressures of the soil elements along the wall in both the damped and undamped models (Figure 45).

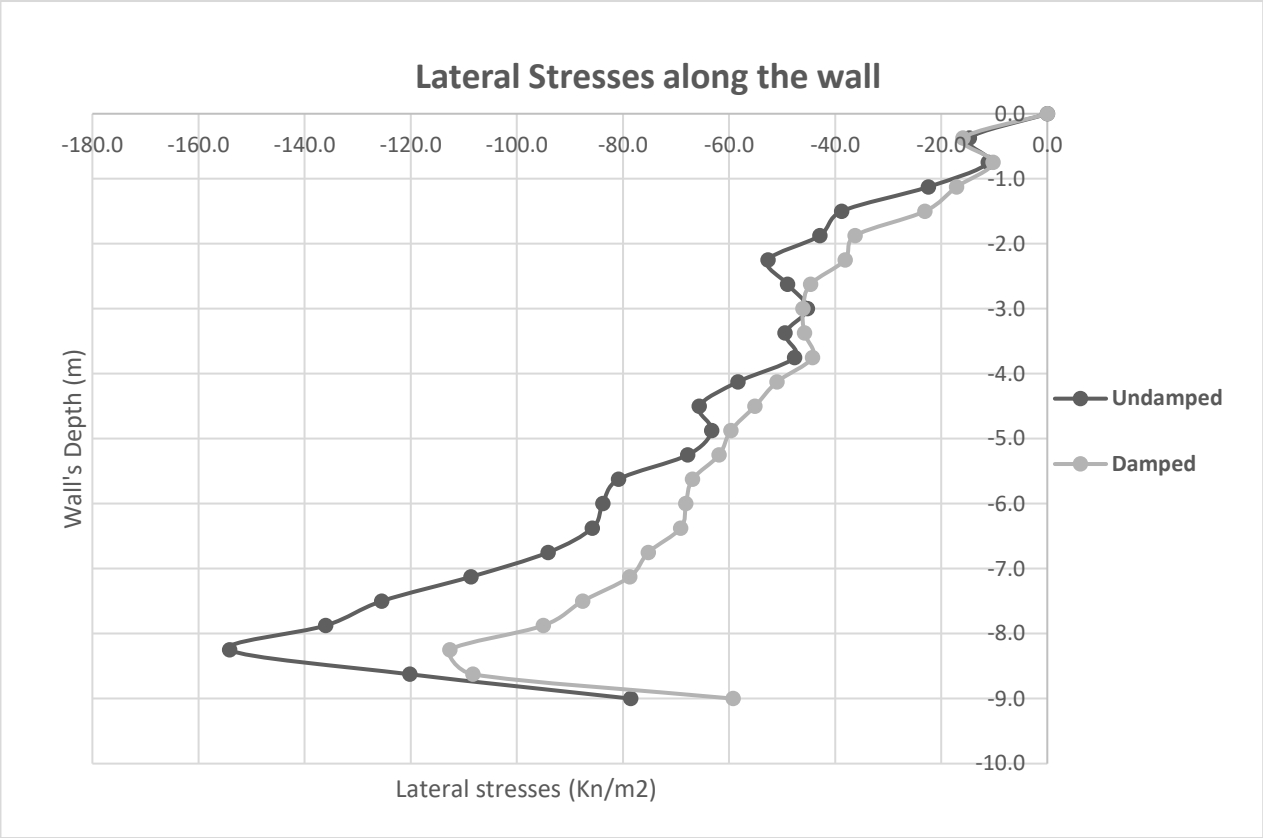

Figure 45 Lateral Stresses along the Left Wall

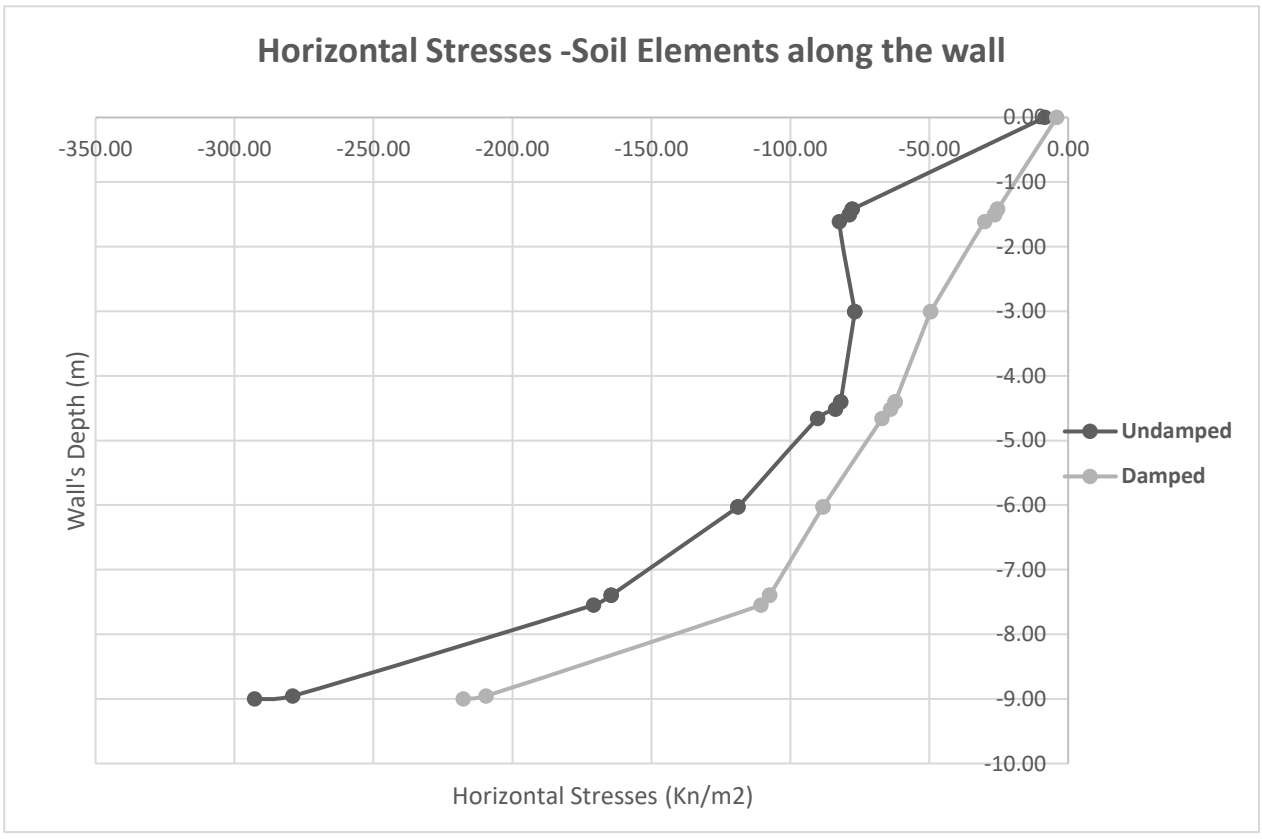

Figure 44 Horizontal Stresses of the soil elements at 0.*4cm* from the wall

Results from figure 44 show a 26.6% reduction in the lateral pressure exerted on the wall at -8.24m depth. This is calculated knowing the lateral pressure exerted on the wall in the case of the damped model was 113.3kn/m2 and 153kn/m2 in the undamped model.

Results from Figure 45 show a 25.4 reduction in horizontal pressure exerted on the soil elements. This is a result of the end horizontal stress of -292.84n/m2 in the undamped model and 218.2kn/m2 in the damped model.

CHAPTER 5

CONCLUSION

5.1 Introduction

In this chapter, the outcome of this research item is summarized, discussed and compared with previous works. This would help up in contributing to future works ideas. The work presented in this thesis aimed at provided a better understanding of the importance of not only incorporating soil damping characteristics in a soil-structure analysis problem but also a medium of incorporating it. Several conclusions were derived from the problem that can be considered as significant findings.

5.2 Overview of the results

Going over the results, a constant favorable effect of damping is seen in terms of its effect on lateral displacement (both and base and roof levels), structural base shear and lateral/horizontal earth pressures. This favorable reduction in such factors doesn't only play an important role in enhancing structural performance but also imposes an economical advantage. Moreover, the parametric analysis prior to analyzing the effects of damping on structural responses assisted in building up a numerical model that captures the significant effects of including damping. Knowing that damping's inclusion becomes remarkable in loose soils while compared to dense soils, in larger earthquake intensities and the importance of incorporating hysteretic damping in addition to Rayleigh, radiation and numerical damping are all factors that provide a better understanding of the soil's damping phenomena.

5.3 Discussion

Results have shown that Rayleigh damping cannot be used as an alternative for hysteretic material damping. However, it can be added to hysteretic damping to provide at least a small amount of damping at small strain levels. Moreover, damping's effect in soils is more significant in loose soils compared to dense sands (12% compared to 6%, respectively).

Damping effects can be beneficial. Considering the preliminary results, damping's effect is favorable in seismic design as its inclusion decreases lateral displacements, ground base shear and lateral/horizontal stresses. This was a general finding in the research and falls in compliance with the literature.

Lateral displacements represent a critical design parameter in the seismic design of buildings. Soil damping being able to decrease this value would result in more economical buildings (in addition to the reduction in base shear and lateral pressures) which is also observed. A final permanent deformation was observed in all models. This is a result of an earthquake of high intensity similar to Loma Prieto earthquake. A larger final permanent deformation in observed in loose sands compared to dense sands.

Moreover, ground base shear turned out to be highly influenced by the dissipation of energy from the soil medium. A higher reduction in base shear within the damped models was seen in those subjected to earthquakes of higher magnitude compared to those with a lower magnitude. A non-zero final base shear is the result of the permanent deformation developed because of the earthquake input motion which was developed as a result of the soil's passive behavior.

Finally, to provide better clarification for the results obtained concerning the effect of damping on the lateral earth or horizontal pressures, an extended model was

developed to have a better understanding of the retaining wall's state in terms of the pressure induced on it. According to the results, damping's effect on horizontal pressures becomes more significant at greater depths. This might be a result of knowing the soil becomes denser with depth hence more dissipation of energy can be observed. A final permanent deformation lead to exerted final pressure. This needs to be further studied to provide a better understanding of the passive behavior of the wall.. Moving back to the main objective, damping can have a major role in reducing horizontal pressure on the retaining walls. An initial induced pressure was also observed as the building was already subjected to pressure due to the settlement of the building (3.8cm).

In conclusion, damping is a remarkable soil characteristic. Its effects are substantial and cannot be limited to this study. Its effects wouldn't only enhance structural performance and help structures withstand larger dynamic loadings but also assist in creating more economical structural systems.

5.4 Future Work

Although this research answers several questions regarding the effect of damping in soil-structure interaction on the seismic design of reinforced concrete buildings, some suggestions regarding future works might be promising.

Taking into consideration the achieved results, wider research implemented on the effect of damping on lateral earth pressure would be favorable. Moreover, research conducted on dwarf structures or considering different unmentioned parameters would also be of significance. In addition, this research would be of great value if conducted on steel structures in place of reinforced concrete members. Finally, it would be interesting to know how the effects would alter using 3D modelling in comparison to the present 2D model.

REFERENCES

Ahmadi, E., Khoshnoudian, F., & Hosseini, M. (2015). Importance of soil material damping in seismic responses of soil-MDOF structure systems. *Soils and Foundations*, 35-44.

Ambrosini, R. (2006). Material Damping vs. Radiation Damping in Soil-structure Interaction Analysis. *Computers and Geotechnics*, 86-92.

Boaga, J., Renzi, S., Deiana, R., & Cassiani, G. (2015). Soil damping influence on seismic ground response: A parametric analysis for weak to moderate ground motion. *Soil Dynamics and Earthquake Engineering 79*, 71-79.

Brinkgreve, R. B., Engin, E., & Engin, H. K. (2010). Validation of empirical formulas to derive model parameters for sands. *Numerical Methods in Geotechnical Engineering*.

Brinkgreve, R., & Vermeer, P. (2015). *Plaxis Manual Version 2015.02.* Delft.

Brinkgreve, R., Kappert, M., & Bonnier, P. (2007). Hysteretic damping in a small-strain stiffness model. *Numerical Models in Geomechanics*, 737-742.

Cruz, C., & Miranda, E. (2017). Evaluation of soil-structure interaction effects on the damping ratios of buildings subjected to earthquakes. *Soil Dynamics and Earthquake Engineering*, 183-195.

Das, B. (2007). *Principles of foundation engineering* . Australia.

Dutta, S. C., & Roy, R. (2002). A critical review on idealization and modeling for interaction among soil–foundation–structure system. *Computers & Structures*, 1579-1594.

Dutta, S. C., Bhattacharya, K., & Roy, R. (2004). Response of low-rise buildings under seismic ground excitation incorporating soil–structure interaction. *Soil Dynamics and Earthquake Engineering*, 893-914.

El Ganainy, H., & El Naggar, M. (2009). Seismic performance of three-dimensional frame structures with underground stories. *Soil Dynamics and Earthquake Engineering*, 1249-1261.

Elchiti, I., Najjar, S., Saad, G., & Nasreddine, N. (2017). Investigation of Active Soil Pressures on Retaining Walls Using Finite Element Analyses. In *Geotechnical Frontiers* (pp. 159-169).

Far, H., Fatahi, B., Ghabraie, K., & Zhou, W.-H. (2015). Evaluation of numerical procedures to determine seismic response of structures under influence of soil-structure interaction. *Structural Engineering & Mechanics*, 27-47.

FEMA, A. (2005). *Improvement of nonlinear static seismic analysis procedures.* Redwoord city.

Hudson, M. I. (1994). *QUAD4M: a computer program to evaluate the seismic response of soil structures using finite element procedures incorporating a compliant base.* California: Center for Geotechnical Modeling, Department of Civil and Environmental Engineering, University of California, Davis, 1994.

Jaber, L., Temsah, Y., El-Mossallamy, Y., & Hajj Chehade, F. (2018). Effect of Soil - Structure Interaction Constitutive Models on Dynamic Response of Multi-Storey Buildings. *Journal of Engineering Science and Technology Review 11 (3)*, 56-60.

Jaber, L., Temsah, Y., El-Mossallamy, Y., & Hajj Chehade, F. (2019). The Effect of Underground Stories on the Dynamic Response of High-rise Buildings. *Advances and Challenges in structural Engineering*, 209-218.

Kausel, E. (2009). Early Historey of Soil–structure Interaction. *Soil Dynamics and Earthquake Engineering 30*, 822-832.

Khosravikia, F., Mahsuli, M., & Ghannad, M. (2018). The Effect of Soil-Structure Interaction on the Seismic Risk to Buildings. *Bulletin of Earthquake Engineering*.

Kramer, S. (1996.). *Geotechnical earthquake engineering.* New Jersey:.

Kuhlemeyer, R. L., & Lysmer, J. (1999). Finite Element Method Accuracy for Wave Propagation Problems. *Journal of the Soil Dynamics Division*, 421-427.

Lysmer, J., & Kuhlemeyer, R. L. (1969). Finite Dynamic Model for Infinite Media. *Journal of the Engineering Mechanics Division*, 859-877.

Mekki, M., Elachachi, S. M., Breysse, D., Nedjar, D., & Zoutat, M. (2014). Soil-structure interaction effects on RC structures within a performance-based earthquake engineering framework. *European Journal of Environmental and Civil Engineering*, 945-962.

Mylonakis, G., & Gazetas, G. (200). Seismic Soil-Structure Interaction: Beneficial or Detrimental? *Journal of Earthquake Engineering*, 277-301.

Newmark, N. M. (1959). A Method of Computation for Structural Dynamics. *Journal of the Engineering Mechanics Division*, 67-94.

Rayhani, M. H., & El Naggar, M. H. (2008). Numerical Modeling of Seismic Response of Rigid Foundation on Soft Soil. *International Journal of Geomechanics*, 226-246.

Saad, G., Najjar, S., & Seddik, F. (2016). Seismic performance of reinforced concrete shear wall buildings with underground stories. *Earthquakes and Structures*, 965–988.

Sri Vinay, N., Amrita, Jayalekshmi,, B., & Shivashankar, R. (2021). Dynamic Soil–Structure Interaction Effects in Integrated Retaining Wall-Building System. In *Geohazard Mitigation* (pp. 403-414).

Tabatabaiefar, H. R., Fatahi, B., Ghabraie, K., & Zou, W. H. (2015). Evaluation of numerical procedures to determine seismic response of structures under influence of soil-structure interaction. *Structural Engineering and Mechanics*, 27-47.

Tsompanakis, Y. (2008). Dynamic interaction of retaining walls and retained soil and structure. In *Computational Structural Dynamics and Earthquake Engineering* (pp. 447-461).

Tsompanakis, Y., Psarropoulos, P., & Katsirakis, M. (2021). Dynamic soil-structure interaction between retaining walls, retaining soil and retained structures. *Bulletin of Earthquake Engineering*.

Zerwer, A., Cascante, G., & Hutchinson, J. (2002). Parameter Estimation in Finite Element Simulations of Rayleigh Waves. *Journal of Geotechnical and Geoenvironmental Engineering*.